Tropospheric ozone over the tropical Atlantic: A satellite perspective

D. P. Edwards,[1] J.-F. Lamarque,[1] J.-L. Attié,[2] L. K. Emmons,[1] A. Richter,[3] J.-P. Cammas,[2] J. C. Gille,[1] G. L. Francis,[1] M. N. Deeter,[1] J. Warner,[1] D. C. Ziskin,[1] L. V. Lyjak,[1] J. R. Drummond,[4] and J. P. Burrows[3]

[1]   We use satellite sensor measurements to obtain a broad picture of the processes affecting tropical tropospheric O_3 production over Africa and the Atlantic in the early part of the year. Terra/MOPITT CO retrievals correlate well with biomass burning fire counts observed by the TRMM/VIRS instrument in Northern Hemisphere savanna regions and allow investigation of the subsequent convection of the biomass burning plume at the intertropical convergence zone and interhemispheric transport. Measurements of NO_2 from the ERS-2/GOME instrument enable identification of two important tropical sources of this O_3 precursor, biomass burning and lightning. Good correlation is seen between NO_2 retrievals and TRMM/LIS lightning flash observations in southern African regions free of biomass burning, thus indicating a probable lightning source of NO_x. The combination of MOPITT CO, GOME NO_2, and TRMM fire and lightning flash counts provides a powerful tool for investigating the tropospheric production of O_3 precursors. These data are used in conjunction with the MOZART-2 chemical transport model to investigate the early year tropical Atlantic tropospheric O_3 distribution using January 2001 as a case study. Inconsistencies between the various tropical tropospheric O_3 column products obtained from EP/TOMS data, and between these products, in situ measurements, and modeling, have led to questions about how the Northern Hemisphere biomass burning is connected to the TOMS derived O_3 maximum in the tropical southern Atlantic. We show that the early year tropical O_3 distribution is actually characterized by two maxima. The first arises due to biomass burning emissions, is located near the Northern Hemisphere fires, and is most evident in the lower troposphere. The second is located in the southern tropical Atlantic midtroposphere, and results from NO_x produced by lightning over southern Africa and South America.   *INDEX TERMS:* 0345 Atmospheric Composition and Structure: Pollution—urban and regional (0305); 0365 Atmospheric Composition and Structure: Troposphere—composition and chemistry; 0368 Atmospheric Composition and Structure: Troposphere—constituent transport and chemistry; 3360 Meteorology and Atmospheric Dynamics: Remote sensing; *KEYWORDS:* MOPITT, GOME, ozone, troposphere, biomass, burning, lightning

1.   Introduction

[2]   There has been considerable interest in the recent literature regarding the apparent Atlantic tropical tropospheric O_3 'paradox' [*Thompson et al.*, 2000, 2001]. The problem can be stated as follows: Most of the northern hemisphere (NH) biomass burning in January and February occurs north of the intertropical convergence zone (ITCZ), while the maximum in most of the satellite-derived tropical tropospheric ozone (TTO) columns is observed in the southern hemisphere (SH) tropical Atlantic, south of the ITCZ. Apart from requiring a mechanism of significant O_3 precursor production, and inter-hemispheric transport across the ITCZ, it is also hard to reconcile these observations with modeling studies which generally show high tropospheric O_3 in regions of intense burning. It is also contrary to the situation later in the year, when the high O_3 amounts which develop in the southern Atlantic in September and October correlate reasonably well with the peak of the biomass burning activity in southern Africa and South America.

[3]   Until recently, tropospheric studies have relied on field campaigns, regular ground-based and aircraft measurements from specific sites, and on an important contribution

[1]National Center for Atmospheric Research, Boulder, Colorado, USA.
[2]Observatoire Midi Pyrénées, Toulouse, France.
[3]Institute of Environmental Physics, University of Bremen, Bremen, Germany.
[4]Department of Physics, University of Toronto, Toronto, Ontario, Canada.

from chemical-transport modeling. Satellite remote sensing offers a way to complement these studies by adding the larger geographical and seasonal context. However, remote sensing of the troposphere presents particular problems. Obtaining a total column retrieval might be possible given a suitable spectroscopic feature, but isolating the tropospheric column can be particularly difficult in the presence of a significant stratospheric contribution to the total column. This is one of the main difficulties faced when inferring tropospheric O_3 and NO_2 columns from satellite sensor measurements. Taking the further step of deriving profile information in the troposphere usually depends on probing the pressure-broadened wings of weak spectral lines with a technique that is capable of high effective spectral resolution and signal-to-noise (S/N). These challenges are only just being met, and the latest data from the currently operational tropospheric sensors, and the prospect of new instruments coming online in the next few years, offers an exciting opportunity to extend our knowledge of global tropospheric chemistry and assess whether these measurements are consistent with our current understanding.

[4] In this paper we examine the satellite evidence that can be utilized in explaining the Atlantic TTO distribution in the early part of the year, and we use the month of January 2001 as a case study. The new sensors allow measurements of tropospheric O_3 and its precursors, CO and NO_2, along with observations of biomass burning fires and lightning flashes to provide further information about processes that affect chemistry. In section 2, we describe the savanna biomass burning in northern Africa in the early part of the year and consider the satellite fire counts from the Tropical Rainfall Measuring Mission Visible and Infrared Scanner (TRMM/VIRS). Section 3 presents the chemistry relevant to the formation of tropospheric O_3, and describes how in situ and satellite observations from the Earth Probe Total Ozone Mapping Spectrometer (EP/TOMS) have led to the discussion of an apparent paradox in that the location of the observed SH O_3 maximum over the tropical Atlantic does not coincide with the biomass burning source region. This is followed in section 4 by a model study using the Model for OZone And Related Tracers (MOZART-2) chemical transport model (CTM) to investigate tropospheric O_3 formation and distribution over the tropical Atlantic. Transport processes at the ITCZ are investigated further in section 5 using CO retrieved from Terra Measurement of Pollution in The Troposphere (Terra/MOPITT) observations as a tracer to help explain the extent to which O_3 and precursors from the fire regions could be transported to the location of the O_3 maximum observed by EP/TOMS. The tropical distribution of NO_2 is investigated in section 6 using measurements from the second European Remote Sensing Satellite Global Ozone Monitoring Experiment (ERS-2/GOME), and this is compared to probable source locations as indicated by the TRMM/VIRS fire counts and lightning flash counts taken by the TRMM/Lightning Imaging Sensor (TRMM/LIS). Conclusions are presented in section 7.

2. Springtime Dry-Season Savanna Burning in Northern Africa

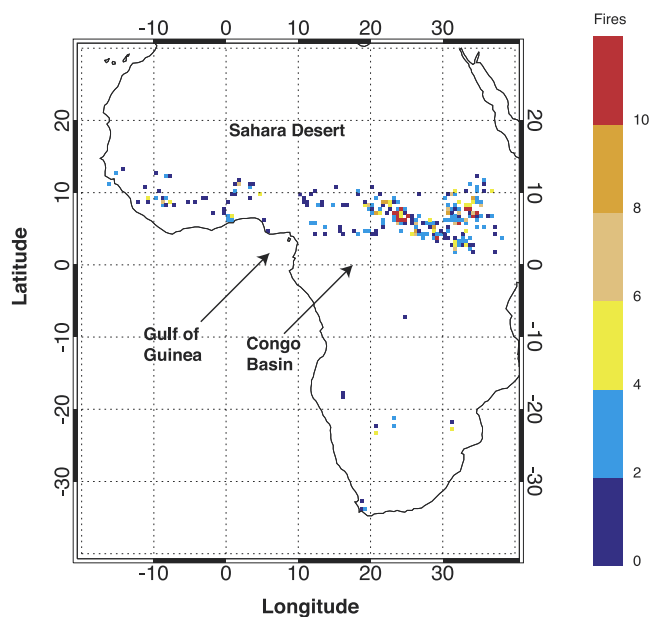[5] It is well-known that biomass burning is a major forcing of tropical tropospheric photochemistry [Andreae,

Figure 1. VIRS/TRMM composite firecount for January 2001. Data resolution is 0.5° longitude × 0.5° latitude.

1991]. Emissions depend on biomass type, meteorology and combustion stage, with large amounts of CO, CH_4, and other hydrocarbons being emitted in the later smoldering stages of a fire [Cautenet al., 1999; Nielsen, 1999].
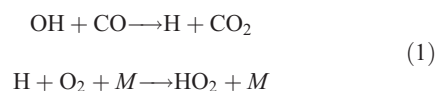
[6] An aid to studying biomass burning emissions is that fire source locations are identifiable over large geographical regions from satellite observations. One such dataset is obtained by the TRMM/VIRS instrument. The TRMM satellite covers a latitude range of ±40° from the equator in about 4 days, and fire counts are reported at a horizontal resolution of 4.4 km × 4.4 km. VIRS identifies fire pixels according to radiance threshold and difference criteria using two thermal channels at 3.75 μm and 10.8 μm [Giglio et al., 2000]. This technique is similar to that used by the Advanced Very High Resolution Radiometer (AVHRR) [Kennedy et al., 1994], and the Along Track Scanning Radiometer (ATSR) [Arino et al., 2001], although a significant difference arises due to the TRMM orbital inclination of 35° which results in all overpass local times being sampled in the course of about one month. Over this period, observations can be made of the complete burning diurnal cycle. However, it is important to note that the TRMM firecount data reported on their web site [http://tsdis.gsfc.nasa.gov/tsdis/Fire/fireintro.html] are not corrected for sunglint effects. We found it necessary to remove spurious counts corresponding to sunglint which occur for observations near local noon. To avoid this problem, the ATSR fire product is based only on nighttime observations. Although this improves the reliability of fire detection, it may introduce a bias since fire activity often peaks in the afternoon [Siegert et al., 1999]. In addition to incomplete satellite coverage, day-to-day variation of fire counts can also be high due to cloud cover obscuring fires. It is therefore most reliable to view composite fire count maps for periods of at least a week.

[7] The composite fire counts for January 2001 over Africa are shown in Figure 1. Counts have been gridded
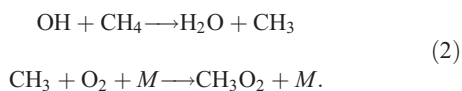
in latitude-longitude bins of $0.5° \times 0.5°$ Northern hemisphere burning in the savanna south of the Sahara Desert, and in the tropical rain forests at latitudes just north of the equator, forms an intense fire band across the continent from December 2000 through to April 2001. This band moves with the dry season as defined by the shifting position of the ITCZ. In general, the burnt area is a zone of high grass production and the majority of these fires are not wildfires, but result from agricultural waste burning associated with subsistence farming. Analyses of the TRMM/VIRS fire count data show that during this period the peak burning region moves from the northern Sahel region southward until January, after which it begins to move north again. This is in agreement with observations made by *Grégoire et al.* [1999] during the Experiment for Regional Sources and Sinks of Oxidants (EXPRESSO) in western Africa in early December 1996. The most intense burning occurred in the second week of January 2001, and was located in the eastern region of southern Ethiopia and Sudan, Central African Republic, Congo, and northern Uganda and Kenya. Fires in western Africa were persistent throughout the season, although January represented a minimum in burning in this region compared to December 2000 or February 2001.

3. Observations of Tropical Tropospheric Ozone

[8] Tropospheric O_3 is important in determining the oxidizing capacity of the atmosphere, both through its direct role, and through its role as a precursor of the hydroxyl radical OH. The latter is formed after photolysis of O_3 and the subsequent reaction of $O(^1D)$ with H_2O, both of which are efficient processes under the conditions of high solar flux and high humidity found in the tropics. In rural areas, oxidation of CO or CH_4 is the main sink of OH through reactions leading to the formation of peroxy radicals ($HO_2 + RO_2$),

$$OH + CO \longrightarrow H + CO_2$$
$$H + O_2 + M \longrightarrow HO_2 + M \tag{1}$$

and

$$OH + CH_4 \longrightarrow H_2O + CH_3$$
$$CH_3 + O_2 + M \longrightarrow CH_3O_2 + M. \tag{2}$$

In clean environments, destruction of O_3 occurs as the peroxy radicals cycle back to OH, for example,

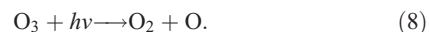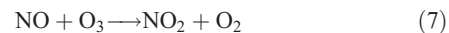$$HO_2 + O_3 \longrightarrow OH + 2O_2. \tag{3}$$

However, in the presence of active nitrogen ($NO_x = NO + NO_2$), from either biomass burning, lightning sources, soil emissions, or industrial pollution, the peroxy radicals react with NO leading to the formation of NO_2,

$$HO_2 + NO \longrightarrow OH + NO_2$$
$$RO_2 + NO \longrightarrow RO + NO_2, \tag{4}$$
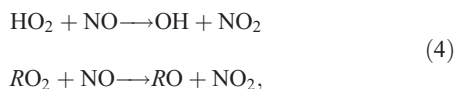
and tropospheric O_3 is formed after NO_2 photolysis

$$NO_2 + hv \longrightarrow NO + O \tag{5}$$

$$O + O_2 + M \longrightarrow O_3 + M. \tag{6}$$
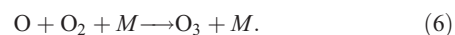
Two other reactions of importance are

$$NO + O_3 \longrightarrow NO_2 + O_2 \tag{7}$$

$$O_3 + hv \longrightarrow O_2 + O. \tag{8}$$

When combined with equations (5) and (6) the above reactions lead to null cycles in terms of O_3 production. Equations (5), (7), and (4), lead directly to the formation of O_3, and define the NO_x partitioning. This is important in determining the NO concentration that is available to react with peroxy radicals to form O_3. Further details of this chemistry are described by *Ridley et al.* [1992] and *Brasseur et al.* [1999].

[9] Assuming high enough UV flux and concentrations of OH, CO, and/or hydrocarbons, NO_x is a rate limiting O_3 precursor [e.g., *Klonecki and Levy*, 1997], except when the concentrations are very high. In the tropical planetary boundary layer (PBL), both NO_x and O_3 react quickly and have lifetimes of a few hours to a day. With convective activity, O_3 and its precursors are lifted to the free troposphere where lifetimes are generally much longer. In the lower free troposphere, NO_x can have a lifetime of several days before it is transformed into a nitrogen reservoir species such as HNO_3 or PAN, while free tropospheric O_3 can have a lifetime of several weeks. Production of tropical O_3 can take place in the polluted PBL and later be convected to the free troposphere, or alternatively, it can be produced directly in the free troposphere following convection of precursors or lightning production of mid-tropospheric NO_x [*Chatfield and Delany*, 1990]. The first process reflects the surface distribution of significant biomass burning sources of NO_x and hydrocarbons, while the second depends more strongly on transport processes. There is also some evidence for free-tropospheric O_3 production following chemical recycling of NO_x from the nitrogen reservoir species [*Tie et al.*, 2001]. The rapid recycling of HNO_3 to NO_x in sulfate aerosols or on soot may be important since both sulfate and soot are produced in biomass burning. *Wang et al.* [1998] found some evidence for the recycling of biomass burning outflow over the tropical south Atlantic during the 1992 Transport and Atmospheric Chemistry Near the Equatorial Atlantic (TRACE-A) campaign. Isentropic transport of O_3 from the lower stratosphere due to Rossby wave breaking is also important at midlatitudes, and possibly over the western tropical Atlantic [*Scott et al.*, 2001].

3.1. In-Situ O_3 Measurements Across the African ITCZ

[10] Evidence for the apparent tropical O_3 'paradox' was presented by *Thompson et al.* [2000]. Measurements taken during the Aerosols99 trans-Atlantic cruise from Norfolk VA, USA, to Cape Town, South Africa, in January−Febru-

ary 1999, showed surface CO concentrations higher by a factor of two north of the equator compared to south, with large peaks near 5°N at about the latitude of the NH biomass burning. The low (0–5 km) and midtroposphere (5–10 km) O_3 concentrations from sondes north of the equator were comparable at about 50 ppbv, with an indication of elevated levels due to a biomass burning plume between the equator and 10°N. South of the equator, where there was no burning, there was a decline in the lower-troposphere O_3 to about 30 ppbv, and an increase in midtropospheric O_3 values with peaks above 60 ppbv, leading to an O_3 'reversal' at the higher altitudes.

[11] A similar behavior was observed from aircraft measurements of O_3 taken during the first Tropospheric Ozone Experiment (TROPOZ-1) [*Marenco et al.*, 1990; *Jonquieres et al.*, 1998], and more recently, during the measurements of O_3 and H_2O by automated equipment on Airbus aircraft operated by commercial airlines, MOZAIC [*Marenco et al.*, 1998]. Figure 2 shows O_3 vertical profiles taken on a MOZAIC flight on 26 February 2001, at takeoff from Brazzaville, Congo (4.37°S, 15.46°E), and on landing at Douala, Cameroon (4.01°N, 9.72°E). At this time of the year, Douala is just north of the ITCZ and at roughly the same latitude as the biomass burning, while Brazzaville is well in the meteorological SH. In the lower troposphere, between 700 and 800 hPa, plume structure (reaching 70 ppbv) is observed in both the profile data from Brazzaville and Douala. In the mid and upper troposphere, the O_3 concentrations at Brazzaville are considerably higher. This is also shown by data taken on the flight transect between the two cities at an altitude corresponding to about 200 hPa. The O_3 concentration is seen to decrease along the flight path heading north. The spikes that are observed near the equator may correspond to convection of O_3 that results from biomass burning in the region of the ITCZ. This is examined further in section 5.2.

3.2. Satellite Observations of Tropical Tropospheric Ozone

[12] Obtaining a tropospheric O_3 product from satellite remote sensing is very difficult due to the overlying stratospheric column, which is some ten times greater than the tropospheric column. Most techniques have relied on subtracting the stratospheric component from the total column to leave the tropospheric column, a method initially employed by *Fishman and Larsen* [1987] using a combination of data from the Stratospheric Aerosol and Gas Experiment (SAGE) and TOMS. Reviews of the various TOMS techniques currently being used and assumptions that they make to determine the overlying stratospheric burden are presented by *Newchurch et al.* [2001] and *Martin et al.* [2002a]. Significant differences (10–20 DU) exist between the current TOMS-based methods. However, most show a zonal wave-one pattern in tropical TTO at this time of year, with a maximum over the Atlantic and a minimum over the western Pacific. This feature is also seen in the total column, but is attributed to the troposphere under the assumption of small O_3 zonal variation in the stratosphere. Of particular interest in this work is the fact that most of the techniques indicate a significant maximum in TTO in the SH tropical Atlantic early in the year, away from the region of NH African burning. In Figure 3 we show the monthly mean TTO column for 1–27
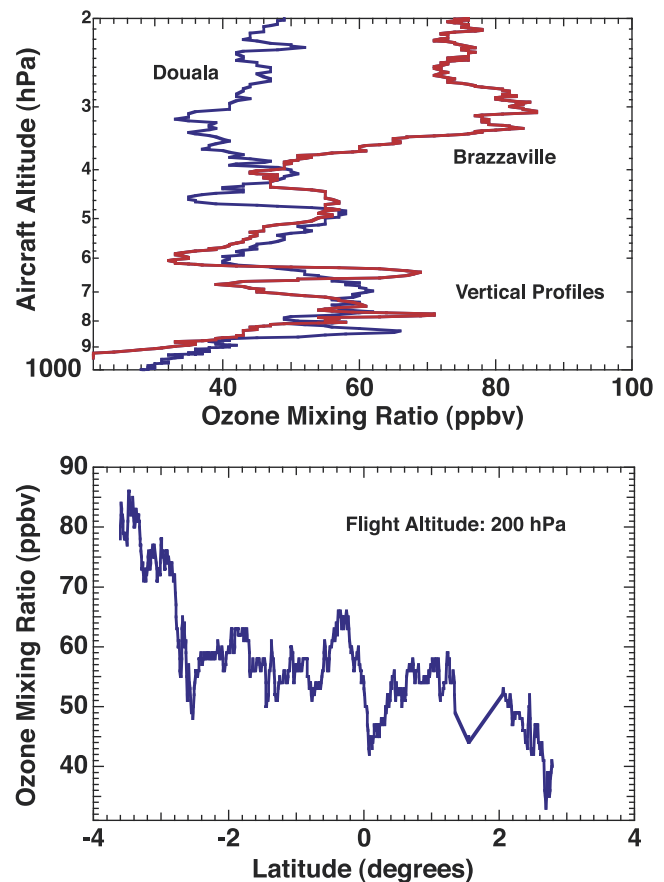

Figure 2. Ozone measurements taken during a MOZAIC flight on 26 February 2001. The top panel shows the vertical profiles on takeoff from Brazzaville, Congo (4.37° S, 15.46°E), and on landing at Douala, Cameroon (4.01° N, 9.72°E). The bottom panel shows the O_3 concentration along the flight transect between the two cities.

January 2001 obtained using the EP/TOMS modified residual method [*Thompson and Hudson*, 1999]. Data are shown for the latitude range over which the retrieval method is considered reliable due to the assumptions that are made about the invariability of O_3 in the tropical stratosphere, and gaps correspond to cloudy regions. It should be noted that recent instrumentation problems affecting the EP/TOMS total O_3 measurements are still being addressed in the TTO data processing, and Figure 3 is presented to qualitatively indicate the position of the derived TTO maximum at this time, rather than its absolute value (Anne Thompson, NASA GSFC, private communication, 2002). This is similar to Figure 4A of *Thompson et al.* [2000], which shows the TTO for 1999 during the Aerosols99 trans-Atlantic cruise, indicative of the fact that the maximum is generally observed at this time of the year. High levels of O_3 are seen below about 5°S and extend from the continents out over the Atlantic. There is also some indication that the region of high O_3 extends southward of the area where retrievals are made.

[13] A number of authors have discussed the low-altitude insensitivity of the TOMS O_3 measurements [*Klenk et al.*, 1982; *Hudson et al.*, 1995; *Fishman et al.*, 1996; *Kim et al.*, 2001; *Martin et al.*, 2002a]. Possible explanations have included the fact that TOMS techniques are adversely
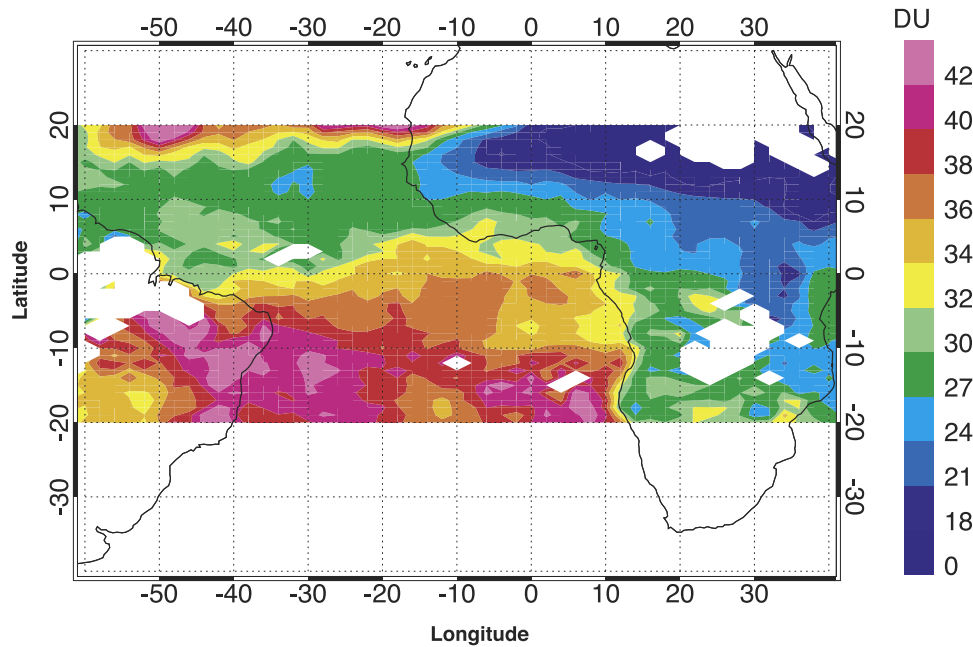
Figure 3. TOMS tropospheric O_3 column average for $1-27$ January 2001, obtained using the modified residual method. Data resolution is $2°$ longitude $\times$ $1°$ latitude.

affected by clouds, which are prevalent near the ITCZ, by desert dust, and by aerosol and haze near fires. The effect of Rayleigh scattering and low surface albedo over land on the TOMS retrieval sensitivity has recently been examined in detail by *Kim et al.* [2001] and *Martin et al.* [2002a]. The TOMS sensitivity to O_3 at 700 hPa is half that at 300 hPa, which makes the retrieval very dependent on the choice of the a priori standard profile that is used to supplement measurement information in the tropospheric column determination. By applying a correction to the standard profile using a CTM, *Martin et al.* [2002a] show that most TOMS TTO products currently underestimate the observed column when the lower tropospheric O_3 is high and overestimate it when the lower tropospheric O_3 is low. Use of this correction in the convective cloud differential (CCD) TOMS TTO method [*Ziemke et al.*, 1998] results in a decrease in the north-south "reversal" in O_3 over the tropical Atlantic during December–February from 20 DU to 10 DU. The SH enhancement is, however, still present. It is interesting to note that another TOMS TTO technique, the scan-angle method [*Kim et al.*, 2001], shows the opposite latitudinal structure to the modified residual and CCD methods early in the year. Instead of an O_3 maximum in the southern tropical Atlantic, this technique produces a maximum in the NH in the vicinity of the biomass burning regions. The scan-angle method utilizes the fact that TOMS measurements taken at different scan and solar zenith angles have different sensitivities to tropospheric O_3, and tends to emphasize O_3 in the lower troposphere. The method also reduces the influence on the retrieved TTO of the SH O_3 maximum which is seen in the total column at this time.

4. Model Studies of the Tropical Tropospheric Ozone Distribution

[14] In this section, we present results of a study using the MOZART-2 CTM to investigate the tropospheric O_3 dis-

tribution over Africa and the tropical Atlantic. In particular, we use the model to determine the relative importance of biomass burning and lightning as sources of NO_x in January 2001 and the consequences that this has for O_3 production. Previous modeling studies have shown that the modeled distribution of tropospheric O_3 and precursors agrees reasonably well with the observed seasonal variation of the African fires [*Hauglustaine et al.*, 1998; *Wang et al.*, 1998; *Galanter et al.*, 2000; *Martin et al.*, 2002a]. This has further added to the apparent O_3 "paradox," because models such as MOZART-2 generally show significant O_3 levels over the NH January fires which are not observed in TOMS TTO products such as those obtained from the modified residual and CCD methods.

[15] MOZART [http://acd.ucar.edu/models/MOZART/] was developed at NCAR and the Max-Planck Institute to study tropospheric chemistry, and a complete discussion of the model and its evaluation is given by *Brasseur et al.* [1998] and *Hauglustaine et al.* [1998]. A description of the updated version of MOZART, the MOZART-2 community model, is in preparation (L. W. Horowitz et al., A global simulation of tropospheric ozone and related tracers: Description and evaluation of MOZART, version 2, submitted to *Journal of Geophysical Research*, 2002). MOZART-2 provides the distribution of 63 chemical constituents (including nonmethane hydrocarbons) between the surface and the upper stratosphere. In this study, we use the model at a horizontal resolution of about $2.8°$ (T42) in both latitude and longitude. The continuity equations for the simulated species account for advection, convection, diffusive transport, surface emissions, photochemical conversions, and wet and dry deposition. The evolution of species due to all physical and chemical processes is calculated with a time step of 20 minutes. For this study, we use analyzed winds provided by the National Center for Atmospheric Research/National Centers for Environmental
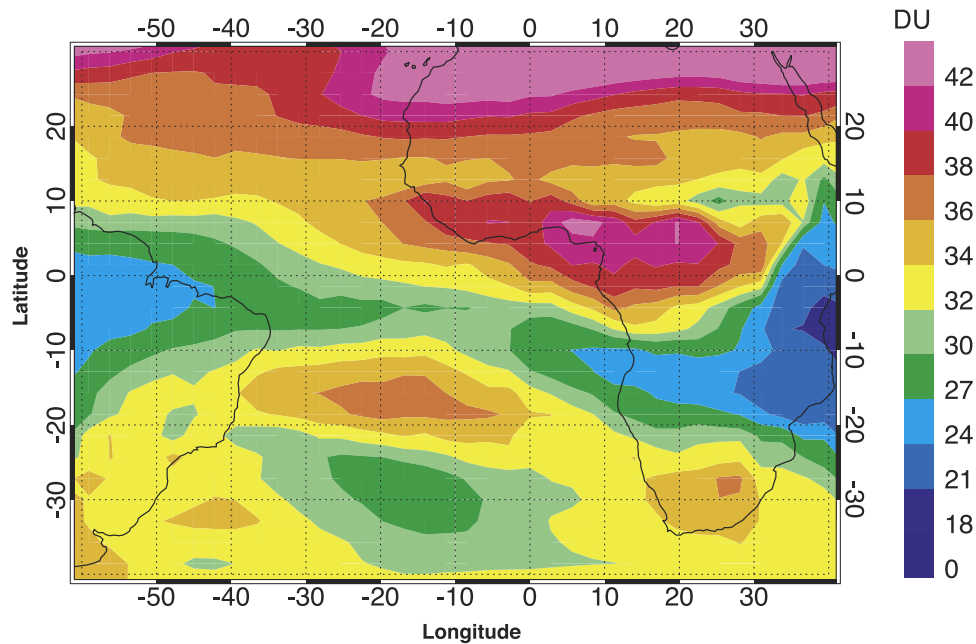
Figure 4. MOZART-2 January 2001 mean tropospheric O_3 column (DU) below 168 hPa.

Prediction (NCAR/NCEP) reanalyses for the year 2000–2001.

[16] Biomass burning emissions in CTMs such as MOZART-2 are usually defined by climatological inventories such as that of *Hao and Liu* [1994]. However, examination of satellite fire counts shows a high degree of interannual variability for a given time period, and this may differ significantly from the climatological average over many years. When comparing measurements of tropospheric gases with model predictions in the tropics, we have found that it is important to redistribute, by month and model spatial grid, the annual CTM climatological biomass burning emissions according to the satellite observed fire counts in order to obtain reasonable agreement between measurement and model. This is particularly important for data assimilation applications of the model.

[17] In this study, we use the ATSR [*Arino et al.*, 2001] fire observations for the 1998–2001 period, [http://shark1. esrin.esa.it/ionia/FIRE/AF/ATSR/], to create a 3 year fires counts climatology. The model climatological source of CO from biomass burning is redistributed according to the monthly ATSR fire counts under the assumption that the constructed 3-year climatology is directly comparable to that of Hao and Liu. To this end, the integral of fire counts over different regions and for forests or grasslands is compared to the integral of the equivalent CO source from Hao and Liu, similar to the work of *Galanter et al.* [2000]. The annual CO amount over each region and land cover type is redistributed on a monthly basis according to the fire counts for the month considered. This ensures both an interannual and monthly variability of the biomass burning source based on the observed fire counts.

[18] The lightning NO_x source is determined as a function of location and time according to the occurrence of deep moist convection. This in turn is determined by the dynamical fields in conjunction with the convection scheme. The lightning NO_x production follows the empirical parameterization of *Price and Rind* [1992]. There is considerable uncertainty regarding the global budget of NO_x from lightning as discussed in detail by *Hauglustaine et al.* [2001], with recent estimates ranging from 0.3–22 Tg N yr^{-1}. The NO_x global lightning emissions inventory in this version of MOZART-2 model is 7 Tg N yr^{-1}. The vertical NO injection between the surface and about 10 km is modeled using the 'C-shape' distribution described by *Pickering et al.* [1998].

[19] Figure 4 shows the MOZART-2 January 2001 mean tropospheric O_3 column below the model 168 hPa level. This distribution can be compared with the TOMS modified residual TTO, Figure 3. Considering the current limitations of the TOMS TTO, reasonable agreement, to within about 5 DU, is obtained between the model and measurement for the O_3 distribution in the tropical south Atlantic. However, the high O_3 over the NH fires, very evident in the model, is largely absent in this TOMS retrieval.

4.1. Ozone From Biomass Burning and Lightning

[20] To investigate the relative importance of the biomass burning and lightning sources of NO_x on the production of tropospheric O_3 at different atmospheric levels, we have performed emission perturbation studies using MOZART-2. In these studies, the total emissions due to biomass burning and due to lightning were separately increased by 10%, and the resulting O_3 fields compared to the unperturbed case. Perturbation runs are probably the safest way to investigate the sensitivity of a trace gas field to a particular emission source, since turning off the source altogether may have other implications for the model chemistry. Small perturbations of 10% lie well within the expected uncertainties or variabilities of both biomass burning and lightning emissions, and we expect the model to respond linearly to the changes. The reference O_3 mixing ratio distributions at 700 and 435 hPa, averaged for January 2001 are shown in Figure 5. The difference in altitude of the NH and SH O_3 maxima is clearly evident.
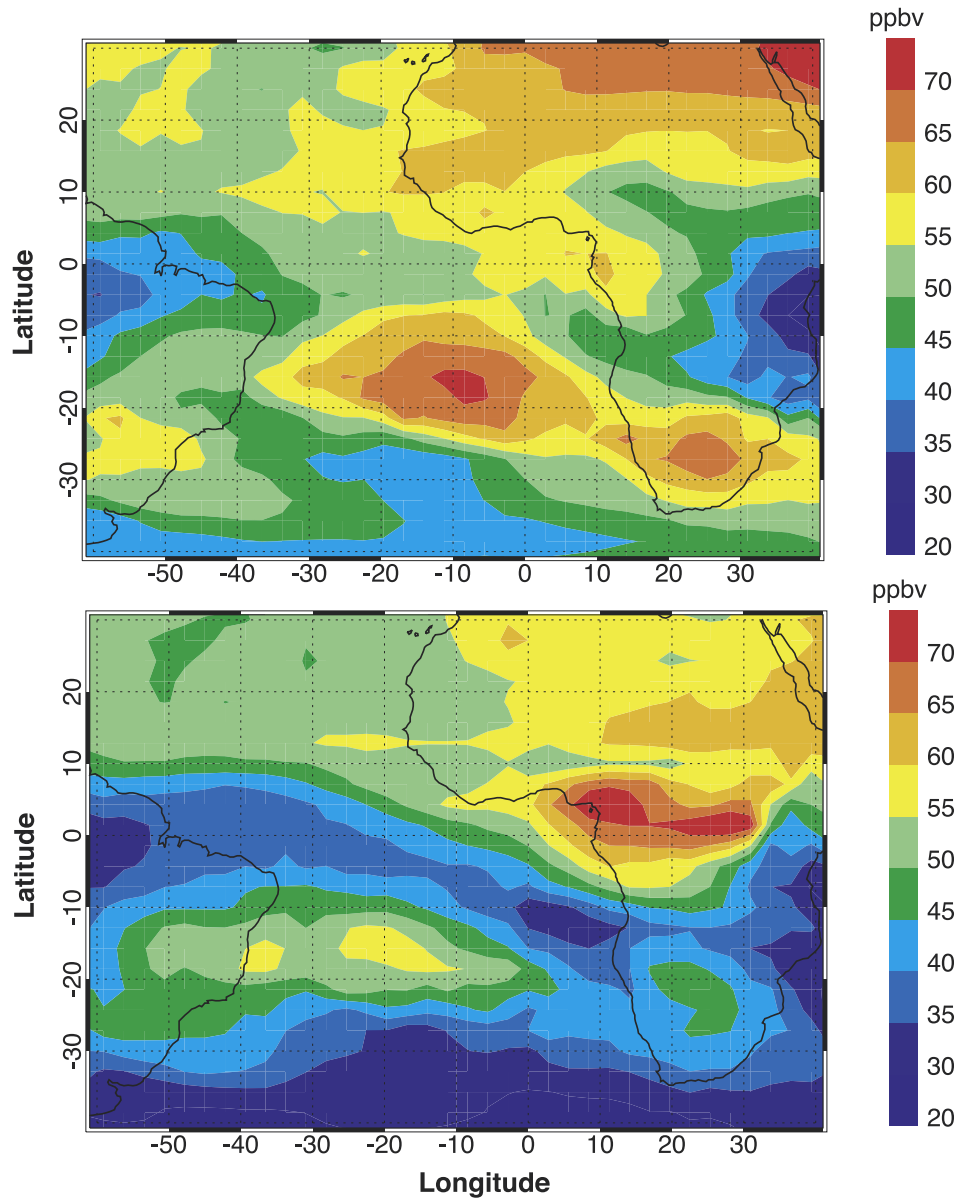
Figure 5. MOZART-2 January 2001 mean O_3 distributions (ppbv) at 700 hPa (bottom) and 435 hPa (top).

[21] Figure 6 shows the change in O_3 mixing ratio at 700 and 435 hPa for a 10% increase in all biomass burning emissions. As expected, the largest perturbation in the O_3 occurs at the lower altitude in the vicinity of the NH biomass burning. This is due mainly to the increased emissions of NO_x, together with CO and CH_4, the latter resulting in higher peroxy radical concentrations after oxidation by OH. At the higher altitude, a significant change in the O_3 concentration occurs to the south of the burning region. The reasons for this will be examined in section 5. The effect of a 10% increase in lightning emissions is shown in Figure 7. At 700 hPa, the perturbation in the O_3 field is small. Even though the lightning "C-shape" vertical distribution used in the model results in significant lower tropospheric NO_x, it is mainly in the form of NO_2. This is due to the efficiency of NO oxidation by O_3 at the higher temperatures and higher O_3 concentrations of the lower troposphere, and the decrease in NO_2 photolysis below clouds. At 435 hPa, however, the NO deposited directly in the midtroposphere means that the lightning emissions perturbation has a significant affect on O_3. The lower temperatures, and lower O_3 and peroxy radical concentrations, at this altitude result in NO_x partitioning favoring NO. The increased lifetime of both NO_x and O_3 results in a significant integrated O_3 production in the plume emanating from southern Africa and South America, and the impact of the lightning perturbation is most evident in the tropical SH in the vicinity of the O_3 maximum observed in the TOMS TTO.

[22] In addition to O_3 contributions to the tropical Atlantic maximum from sources due to the transport of aged lower and midtropospheric air from the NH, and from a lightning NO source, *Thompson et al.* [2000] also suggested that the subsidence of stratospheric air may be important. To
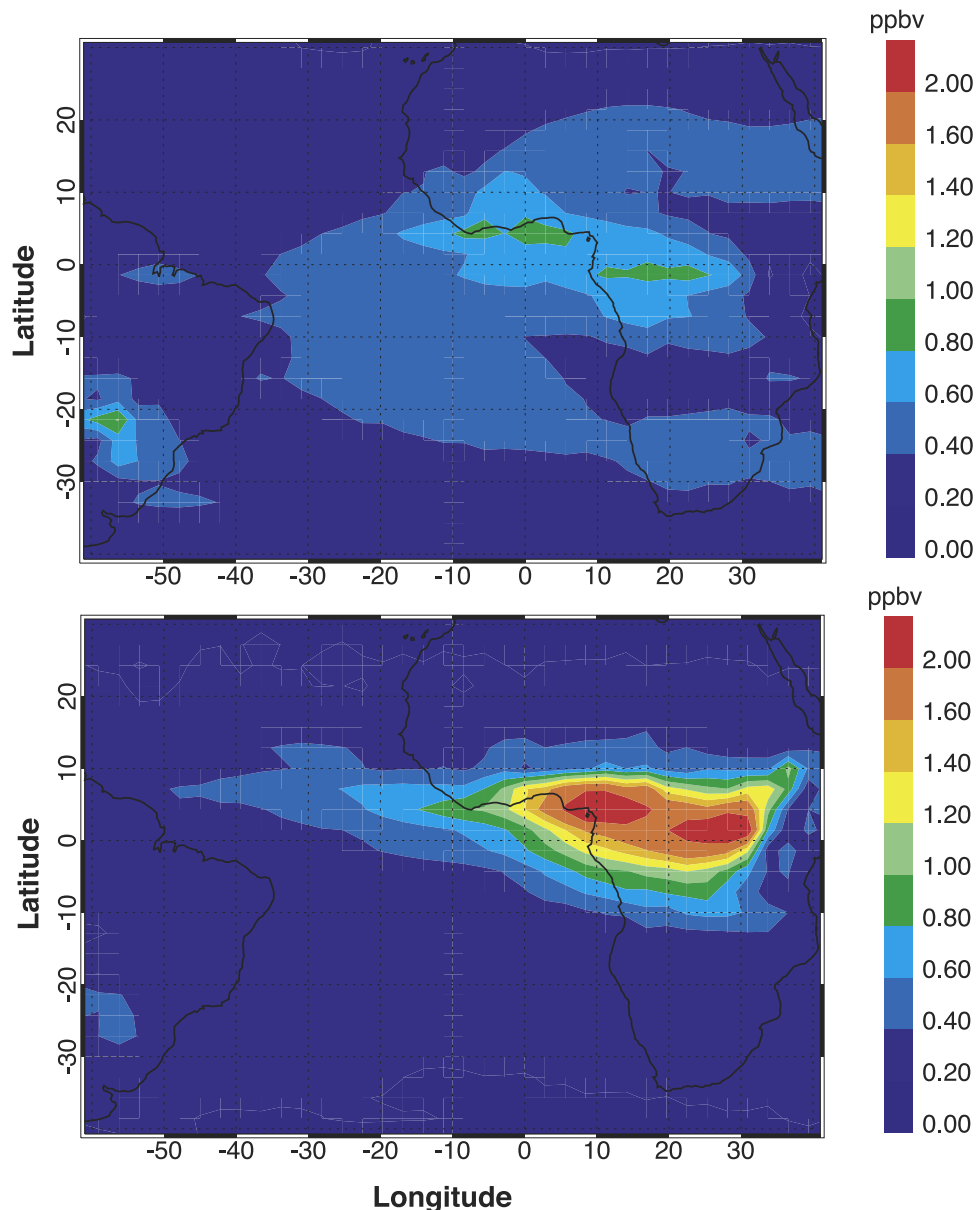
Figure 6.   MOZART-2 January 2001 mean O_3 distribution perturbations (ppbv) at 700 hPa (bottom) and 435 hPa (top) for a 10% increase in all biomass burning emissions.

investigate this, we have performed a study using a tracer of stratospheric O_3 in MOZART-2. This indicates that at the location of the tropical Atlantic maximum, the fraction of O_3 with a stratospheric origin is less than 15% of the 435 hPa total shown in Figure 5, the majority of which results from lightning as described above. The stratospheric contribution is a minimum in this region compared with higher latitudes in general, with the stratospheric contribution in the southern tropics being less that the contribution in the northern tropics.

[23]   This model study suggests that the early year tropical O_3 distribution is actually characterized by two maxima. The first arises due to biomass burning emissions, is located near the northern hemisphere fires, and is most evident in the lower troposphere. In the next section we aim at explaining the MOZAIC aircraft in situ O_3 measurements in terms of transport from this region. The second O_3 maximum is located in the southern tropical Atlantic mid-troposphere and results mainly from lightning NO_x produced over southern Africa and South America. In general, the TOMS TTO products reflect this second maximum more strongly due to the increased retrieval sensitivity at higher altitude. In the discussion that follows, we present further evidence for this conclusion using satellite sensor measurements.

5.   Transport of Biomass Burning Emissions

[24]   In this section, we investigate in detail the transport of biomass burning emissions from the NH fire region and the impact that this has on the observed O_3 distribution. For this purpose, we use CO as a tracer of the emissions. Biomass burning represents the strongest source of CO in the tropics, and this gas is also an important precursor of
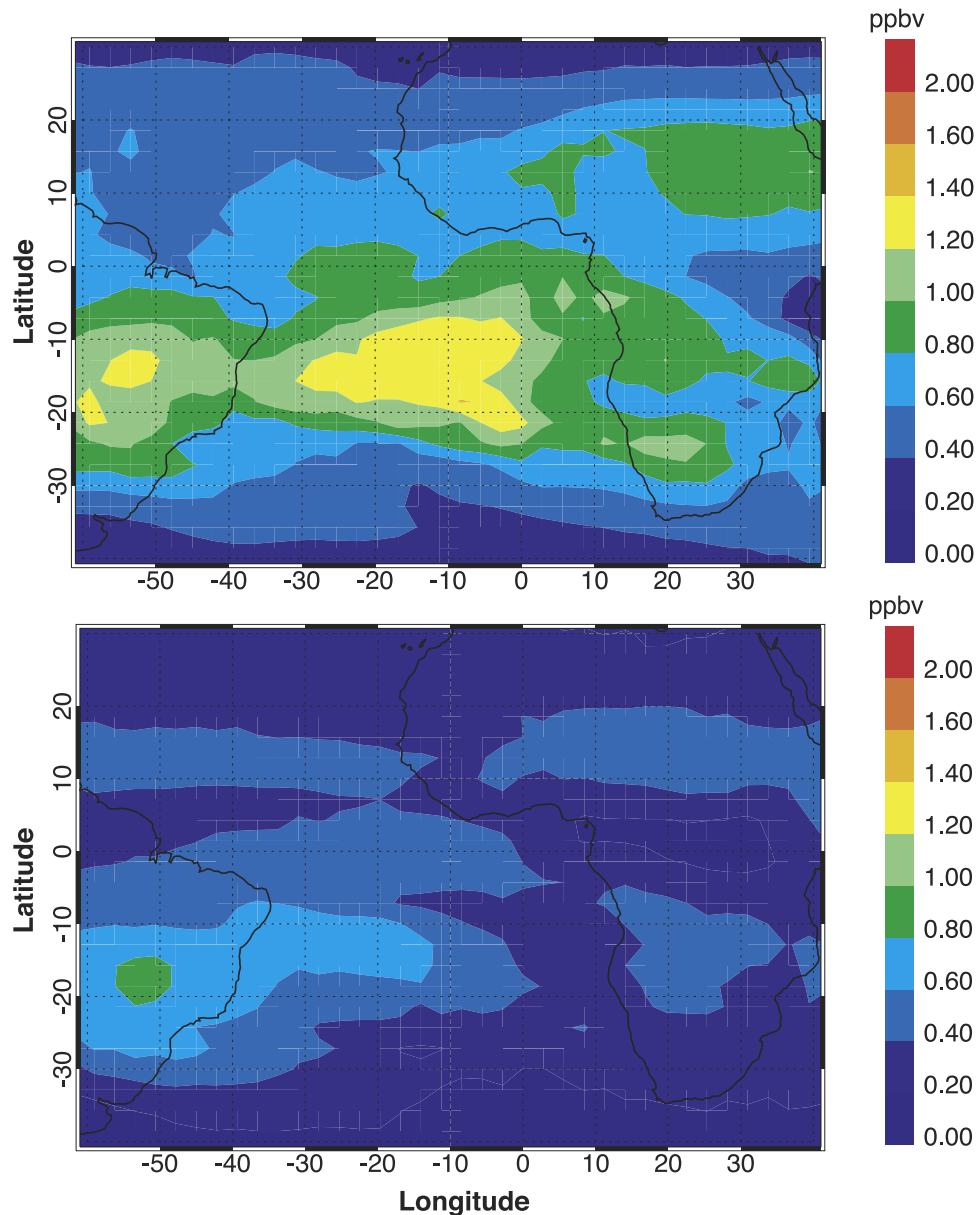
Figure 7.   MOZART-2 January 2001 mean O$_3$ distribution perturbations (ppbv) at 700 hPa (bottom) and 435 hPa (top) for a 10% increase in lightning emissions.

tropospheric O$_3$. The main sink of CO in the troposphere is oxidation by atmospheric OH, and as CO levels rise, they affect the abundance of OH. The resulting CO lifetime is between a week and two months depending on location and season. This is long enough for it to be transported without becoming evenly mixed, therefore making it a useful tracer for studying tropospheric advection and convection processes.

5.1.   The Terra/MOPITT Experiment

[25]   Carbon monoxide is one of the few tropospheric gases that can be successfully monitored from space at the present time. The importance of biomass burning as a source of CO was first seen from space by the Measurement of Atmospheric Pollution from Satellites (MAPS) experiment [*Reichle et al.*, 1990; *Connors et al.*, 1996]. This

instrument measured high levels of tropical midtroposphere CO during two Space Shuttle flights in April and October 1994. High CO was particularly evident during the October flight, and a strong positive correlation was found with tropospheric O$_3$ [*Watson et al.*, 1990].

[26]   The goal of the joint Canadian-US Terra/MOPITT experiment [http://www.eos.ucar.edu/mopitt/] is to provide the first, long term, global measurements of CO and CH$_4$ in the lower atmosphere, and the instrument represents a significant advance in the application of space-based remote sensing to global tropospheric chemistry research. MOPITT is a thermal and near-IR nadir-viewing gas correlation radiometer, and the instrument and measurement technique are described in detail by *Drummond* [1992], *Pan et al.* [1998], and *Edwards et al.* [1999]. The satellite is in a Sun synchronous orbit with a 1030 equator local crossing time.

MOPITT uses a cross-track scan which allows for an almost complete sampling of the Earth's surface in about 3 days, with individual pixels of 22 km × 22 km horizontal resolution. The CO Level 2 (retrieved product) data that we use in this paper come from the first year of operation, during which the instrument had eight operational channels. We use the retrieved CO mixing ratio profiles from data Version 3, which are reported at seven levels (surface, 850, 700, 500, 350, 250, 150 hPa) through the troposphere with a precision of about 10%. It is important to note that the mixing ratios reported at a given level reflect the vertical resolution of the measurement as defined by the retrieval averaging kernels [see Rodgers, 2000] which are reported as part of the standard Level 2 product. Preliminary reports on the validation of the Version 3 data are given by Deeter et al. [2002] and Emmons et al. [2002].

[27] The global mean CO mixing ratio at 700 hPa for a representative week at this time of year, 20–27 January 2001 is shown in Figure 8. The importance of biomass burning as a source of CO over northern equatorial Africa in the global context is readily apparent. The CO mixing ratios over Africa at 500 and 350 hPa are shown in Figure 9. White areas on these plots indicate the locations of persistent clouds over the days sampled. The current MOPITT retrieval algorithm uses information from thermal infrared measurements, and the low thermal contrast between the Earth's surface and the lower atmosphere results in an inherently low sensitivity to CO in the PBL. For this reason, the lowest level shown here is at 700 hPa, and data from this level should not be arbitrarily extrapolated to the surface. Plumes are observed after they have reached the free troposphere, and the observed location may be some distance away from the source region. Despite this fact, the northern extent of the CO plume at the 700 hPa level is seen to correlate reasonably well with the fires in the NH savanna region as indicated in Figure 1. There is also indication of strong convection and net southern transport from the burning region across the equator and into the Gulf of Guinea. The extent of the southern transport is greater at the higher levels, with significant CO plumes from the burning region having reached as far south as 30°S at 350 hPa. We note that this southern transport at high altitude is also reproduced in the corresponding MOZART-2 CO field simulation (not shown) and matches well with the position of the maximum in the 435 hPa O_3 distribution shown in Figure 5.

5.2. Transport at the ITCZ

[28] The CO distributions shown in Figures 8 and 9 suggest strong convection at the ITCZ with subsequent interhemispheric transport. A schematic of this process is shown in Figure 10. Topography and dry convection are important in raising the biomass burning emissions out of the PBL. A further indication of how the biomass burning CO plumes form in the free troposphere can be obtained from trajectory analysis. Forward trajectories calculated using a model [Lyjak and Smith, 1987] driven by NCAR/NCEP reanalysis winds are shown in Figure 11. Here the trajectories have been initialized over the positions of the maximum TRMM/VIRS fire observations (Figure 1). An initialization altitude of 3 km was used since this model does not include a description of subgrid scale processes

such as convection out of the PBL, although the resulting trajectories are not particularly sensitive to this choice. The trajectories indicate that emissions from the region of maximum burning in eastern Africa are generally transported southwest by the prevailing Harmattan flow to the ITCZ, which was located just north of the equator in January 2001. Here they are lofted as the Harmattan meets the incoming cool monsoon air from the Atlantic. These trajectories end up over southern central Africa or out in the Gulf of Guinea, in agreement with the MOPITT CO distributions. Emissions from the fires in western Africa are seen to be advected westward out into the Atlantic, suggesting that the ITCZ in this region presents a stronger barrier to interhemispheric transport. Once in the free troposphere, the CO from west Africa forms a strong plume that is caught in the tropical Easterlies. MOPITT data show that this plume is persistent during the months December 2000– April 2001, and that long-range transport carries CO to South America, landing along the coast from Venezuela to northern Brazil. Part of this plume then crosses South America to the Pacific Ocean, while part is circulated over Amazonia. It is interesting to compare the surface CO in-situ measurements at Ascension Island (8°S, 14°W) during January 2001, which were about 50 ppbv, with the corresponding MOPITT 700 hPa CO retrieval of about 140 ppbv over the same location, Figure 8. The higher mixing ratios measured by MOPITT suggest that once out over the southern tropical Atlantic, the African biomass burning plume is confined to the free troposphere. This is consistent with the lower surface CO values recorded mid-Atlantic south of the equator compared to north of the equator during the Aerosols99 cruise [Thompson et al., 2000]

[29] There is a significant southward gradient to the ITCZ with altitude at this time which is important in producing a net southern transport of the biomass burning emissions. In Figure 12 we have used the meeting of the northward and southward flows of the January 2001 monthly averaged meridional wind from the NCEP reanalysis to indicate the approximate position of the ITCZ at this time. At the surface, this forms a wavy line across the continent around 5°N, just south of the fires as indicated in Figure 1. This variation in the ITCZ position reflects the influence of the African Easterly Jet (AEJ) instability which results in movement of the ITCZ over relatively short time periods. As a result, areas of biomass burning that at one time are located north of the ITCZ may at another time be located in the meteorological SH, and emissions may then be transported southward by local circulations. This was observed by Cautenet al. [1999] in their analysis of the EXPRESSO CO measurements. They concluded that the high levels of CO that were observed over the equatorial rain forests were the result of low-altitude southern transport of northern emissions within the monsoon flow. The AEJ also plays an important role in the westward transport of emissions from the fires in the east of the continent. At 700 hPa, the line where the meridional winds meet shows a distinct southern gradient with respect to the surface position, especially in the region of the Congo Basin. Further evidence of the strong convection in this area is provided by the corresponding outgoing longwave radiation (OLR) map, where low values indicate high clouds. Detrainment of the burning emissions after convection to the divergence
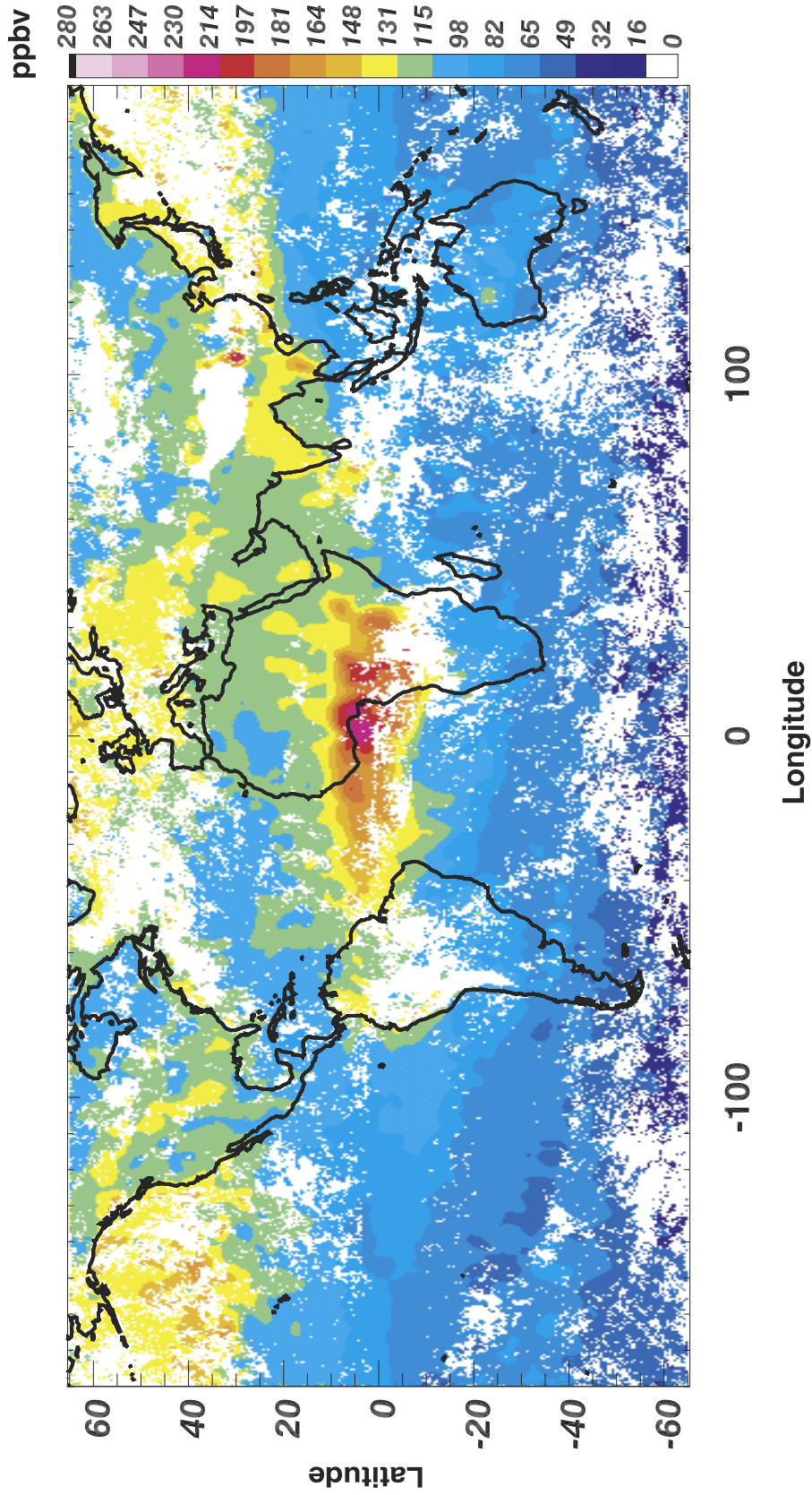
Figure 8. MOPITT CO (ppbv) global mean distribution at 700 hPa for 20–27 January 2001. Data resolution is 0.5° longitude × 0.5° latitude.
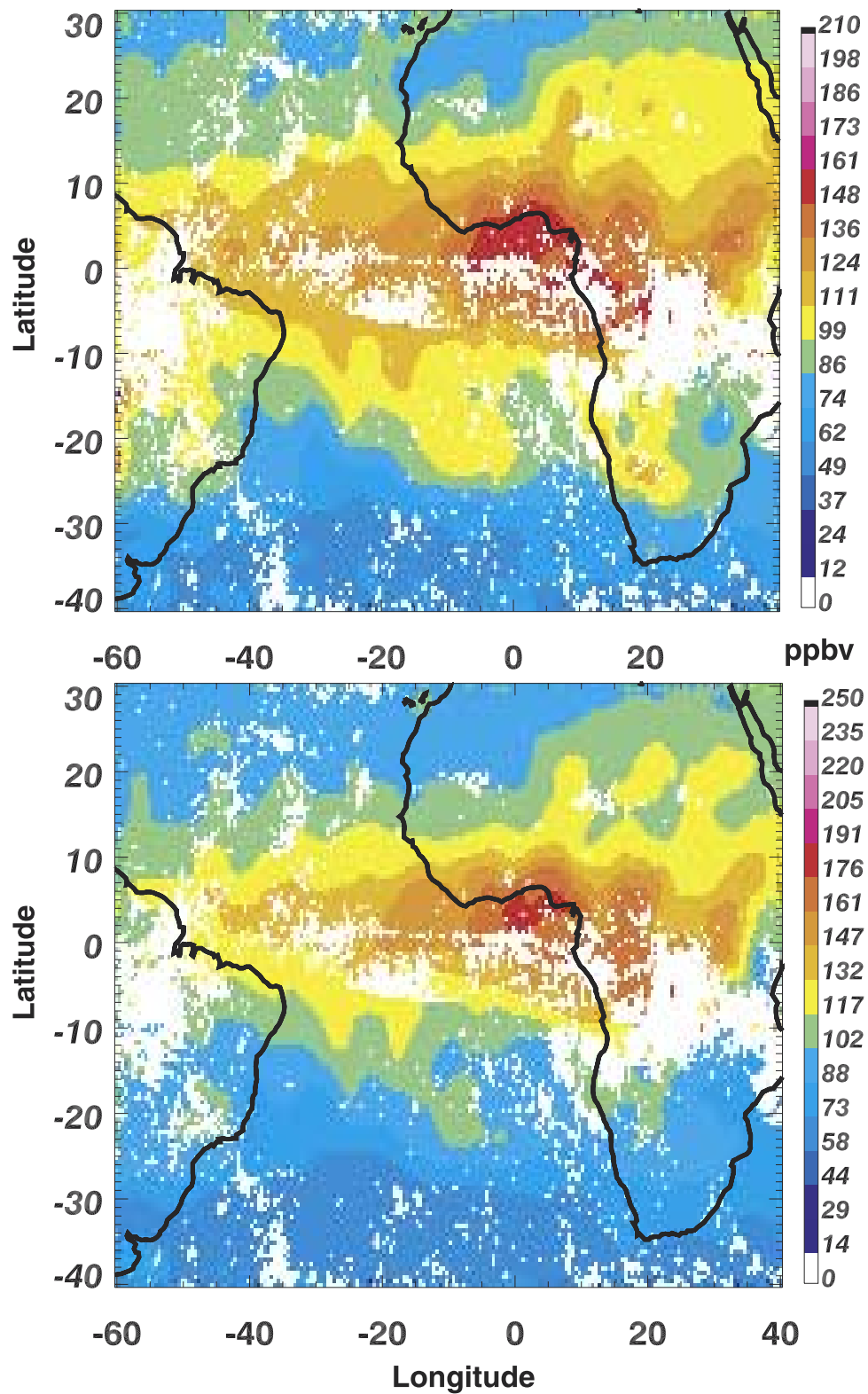
Figure 9. MOPITT CO (ppbv) distributions at 500 hPa (bottom) and 350 hPa (top). Mean values for the period 20–27 January 2001. Note changes in scale. White areas indicate cloud. Data resolution is 0.5° longitude × 0.5° latitude.
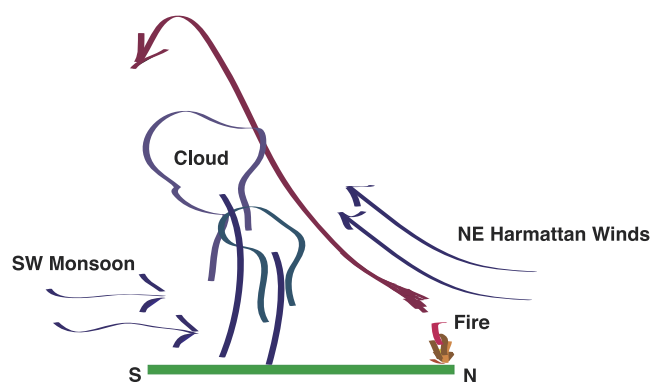
Figure 10. Schematic showing large scale uplift of biomass burning emissions in the vicinity of the ITCZ.

zone around 300 hPa would lead the way for subsequent descent in the SH.

[30] An indication of the convective processes affecting the biomass burning emissions can be obtained directly from the MOPITT profile data. Figure 13 shows the latitudinal CO cross-section as a function of altitude corresponding to the CO distributions shown in Figures 8 and 9. The MOPITT data at the standard retrieval levels have been interpolated in the vertical. The figure shows an average

over the longitudinal range $10°-14°E$, chosen to encompass the MOZAIC flight track shown in Figure 2. The data are not shown below 700 hPa because of the lower sensitivity of the MOPUITT measurement. High CO concentrations are seen in the lower troposphere near $5°N$, at about the same latitude as the peak burning in eastern Africa. With increasing altitude, the peak in the CO concentration is seen to shift southward. The areas of missing data indicate the positions of persistent clouds at this time when retrievals were not possible. The presence of cloud also indicates possible strong convection, and higher values of CO are seen at the upper altitudes surrounding the cloud positions. This is often observed in the MOPITT CO profile data and demonstrates the utility of these measurements for studying convection. In agreement with the trajectory analysis, the upper troposphere CO maximum occurs south of the equator, showing that at high altitude the emissions transported to this region from the fires in eastern Africa are more important in determining the CO distribution than are the emissions from the fires in western Africa, which are relatively less numerous. This vertical distribution is consistent with the aircraft CO measurements made over the Ivory Coast during the TROPOZ 1 campaign [*Jonquieres et al.*, 1998].

[31] The biomass burning emissions and resultant O_3 form what is essentially a low to midtroposphere plume,
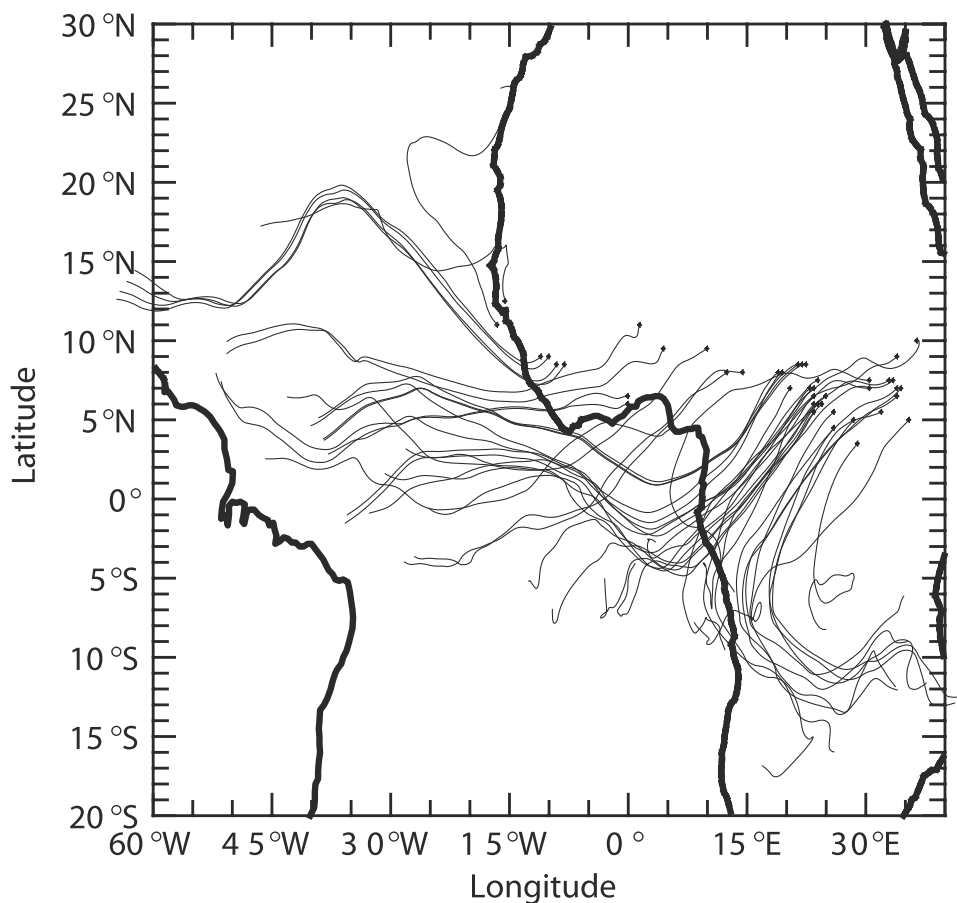

Figure 11. Seven-day trajectories calculated using NCEP winds for $15-22$ January 2001. Positions of trajectory initialization were defined by the locations of TRMM/VIRS fire observations for an injection altitude of 3 km.
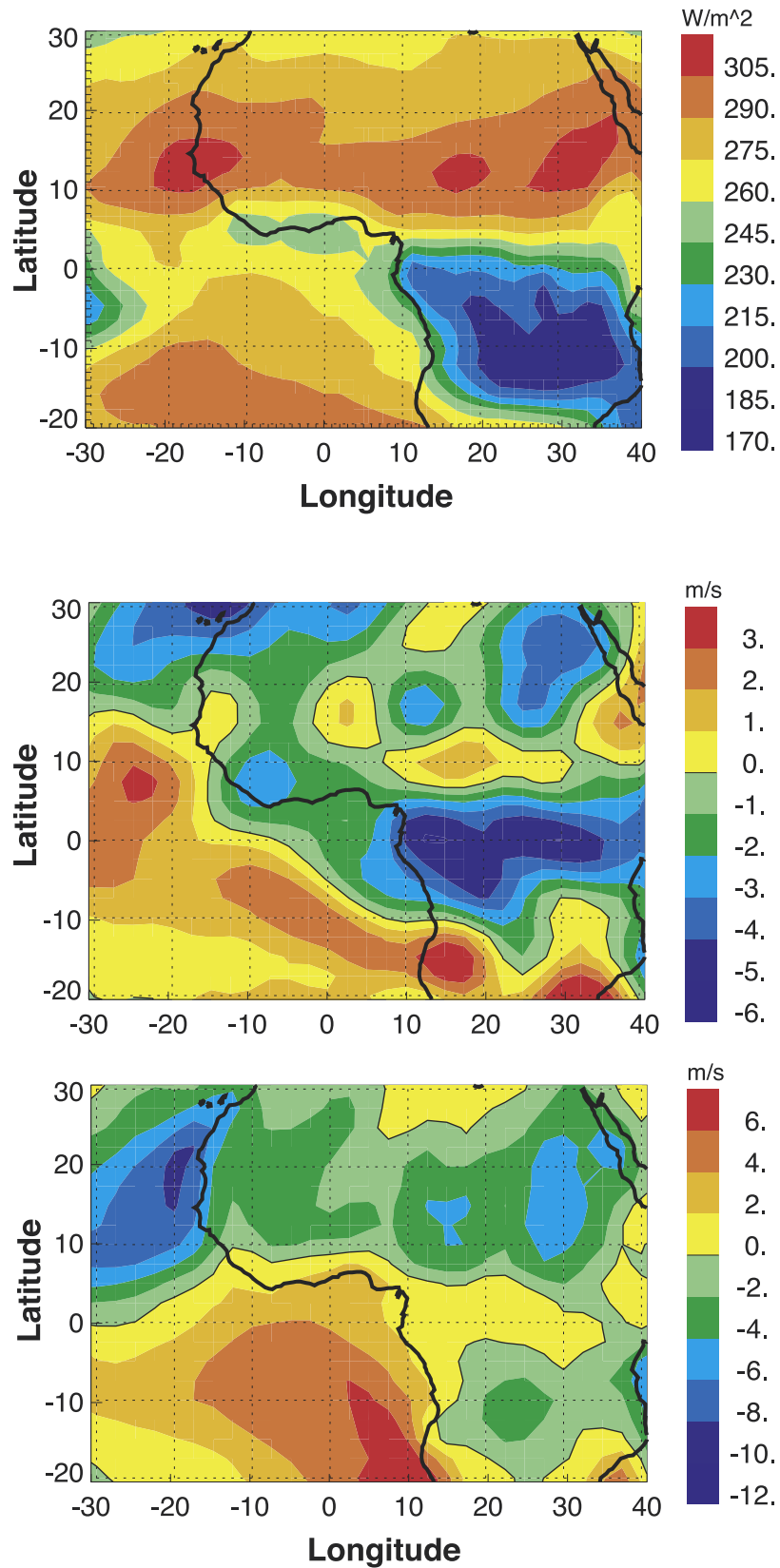
Figure 12. ITCZ mean position in January 2001, as indicated by surface (bottom) and 700 hPa (middle) meridional wind, and by OLR (top). This shows the southward slant of the ITCZ with altitude. NCEP reanalysis and OLR data provided by the NOAA-CIRES Climate Diagnostics Center, Boulder, Colorado, USA, from their Web site at http://www.cdc.noaa.gov/.
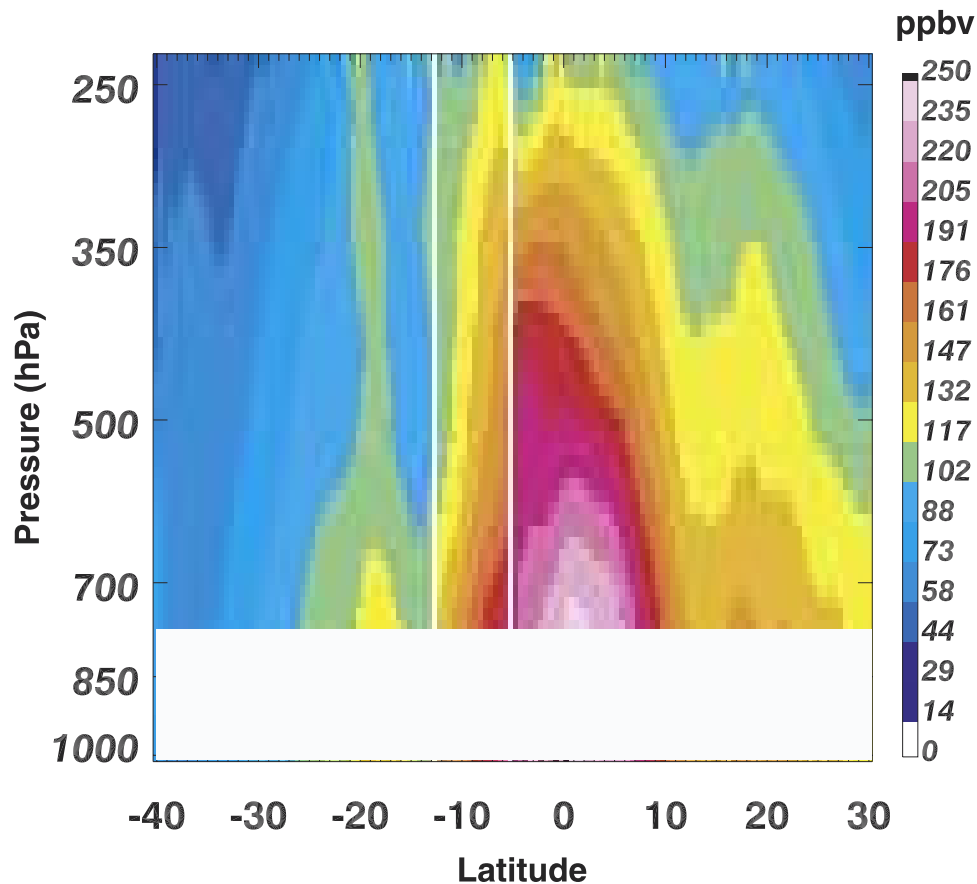
Figure 13. Latitudinal cross-section of MOPITT CO (ppbv) with altitude for the last week of January 2001. Mean values are shown over the longitudinal band 10–14°E. White areas indicate cloud. Data are not shown at the lower levels where the MOPITT measurement sensitivity is low. Data resolution is 0.5° in latitude with linear interpolation between the MOPITT retrieval levels.

extending to about 10°S, with maximum values below about 500 hPa. Within the plume, we obtain a reversal in the CO latitudinal gradient with altitude. Because of increased lifetime, the elevation of burning emissions to the free troposphere is important for long range transport of O_3. Assuming that O_3 and other precursors follow the observed CO distribution, the latitudinal gradient in the mid and upper troposphere CO explains the O_3 gradient observed by the MOZAIC flight.

[32] Figure 14 shows the 24–27 February 2001 MOPITT mean CO distribution at 250 hPa in the region of the 26 February 2001 MOZAIC flight from Brazzaville to Douala. High values of CO are seen near Brazzaville, and decrease north toward Douala, in agreement with the latitudinal variation in the O_3 in situ measurement shown in Figure 2. Note also that the high CO values do not extend much further south than Brazzaville, which is at the southern edge of the biomass burning plume at this time. This analysis also helps explain the peak in the 5–10 km O_3 concentration observed during the Aerosols99 cruise at about 5°S [see *Thompson et al.*, 2000, Figure 2]. It would not, however, explain the broader midtropospheric O_3 maximum observed from 15° to 25°S. While biomass burning may make a contribution to the northern edge, between 5°S and 10°S, of the SH tropical Atlantic midtroposphere O_3 observed by TOMS, it seems unlikely that

it is a significant source of the O_3 at the maximum, which is located further south.

6. The Role of Lightning

[33] Lightning is a major source of tropospheric NO_x, and is estimated to be the dominant (50% or more) source for most of the year between 30°S and 30°N above 500 hPa [*Lamarque et al.*, 1996; *Levy et al.*, 1999]. A conclusion of the MOZART-2 modeling study in section 4 is that O_3 formed in the mid and upper troposphere as a result of lightning over continental southern Africa is advected westward into the Atlantic, so producing the early year SH maximum in the observed TOMS TTO. This mechanism has also been suggested as being important by a number of authors including *Thompson et al.* [2000] and *Hauglustaine et al.* [2001]. In this section, we examine the available remote sensing evidence for significant deposition of midtroposphere NO_x over southern Africa and South America.

6.1. The ERS-2/GOME Experiment

[34] The ERS-2/GOME instrument [*Burrows et al.*, 1999] [http://www.iup.physik.uni-bremen.de/gome/] measures total column NO_2 from which an estimate of the tropospheric column variation can be made [*Velders et al.*, 2001;
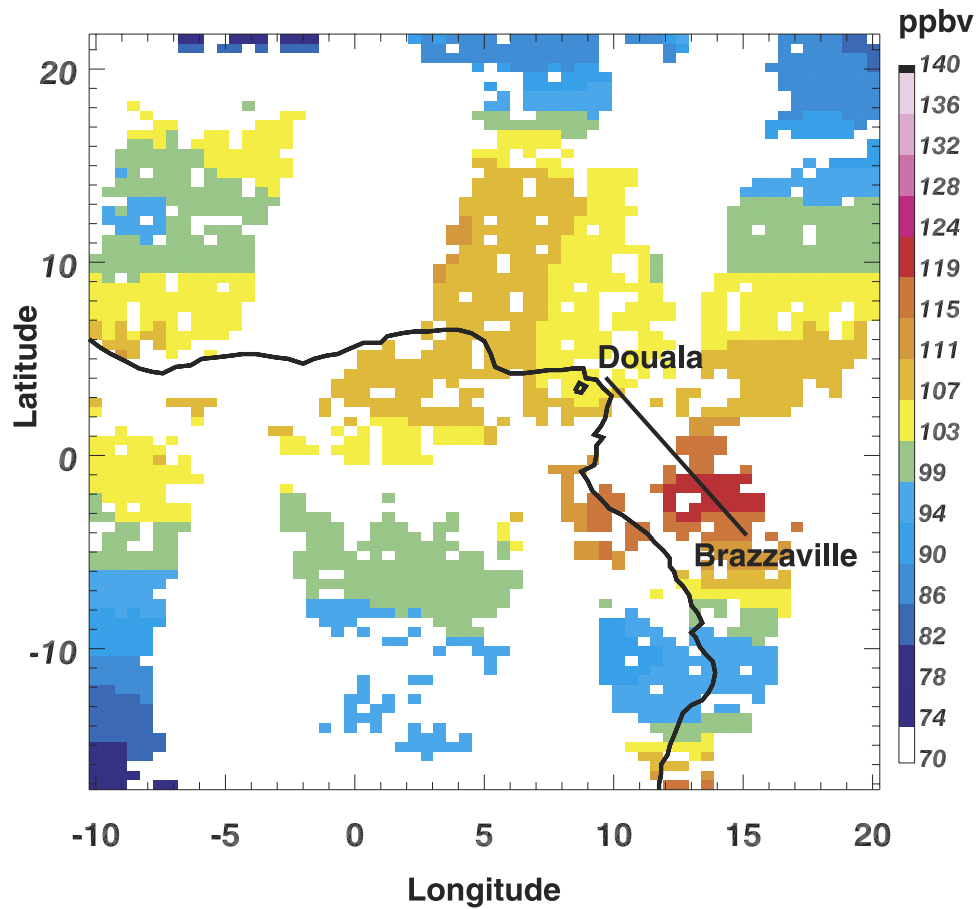
Figure 14. MOPITT CO (ppbv) distribution at 250 hPa. Mean values for the period 25–27 February 2001. White areas indicate cloud. Data resolution is 0.5° longitude × 0.5° latitude. Also indicated is the MOZAIC 26 February 2001 flight track between Brazzaville, Congo (4.37°S, 15.46°E) and Douala, Cameroon (4.01°N, 9.72°E).

Leue et al., 2001; *Richter and Burrows*, 2002; *Martin et al.*, 2002b]. GOME is a nadir-viewing grating spectrometer utilizing reflected solar radiation. A differential optical absorption spectroscopy (DOAS) retrieval [e.g., *Platt*, 1994] is used in which slant column densities are converted to vertical column densities using a calculated air-mass factor. This requires very accurate forward modeling and depends on the vertical NO_2 profile, aerosol loading, cloud cover, and scattering albedo. In contrast to the MOPITT CO retrievals presented here, the GOME NO_2 measurements are reasonably sensitive to the lower troposphere. The satellite is in a Sun synchronous orbit with a 1030 equator local crossing time. GOME has a pixel size of 320 km × 40 km, and achieves global coverage in about 3 days. Retrieval of tropospheric NO_2 is based on the assumption that the stratospheric component of the total column is longitudinally homogeneous for a given solar zenith angle and that the remote maritime troposphere is fairly clean. This allows the zonally invariant stratospheric column to be estimated leaving the varying tropospheric component. Currently, the monthly average product is most reliable due to increased measurement density and improved S/N ratio over many days.

[35] The four main sources of NO_2 over Africa are from biomass burning, lightning, soil, and industrial emissions.

The January 2001 mean GOME residual tropospheric NO_2 vertical column obtained using the retrieval method described by *Richter and Burrows* [2002] is shown in Figure 15. This can be compared directly with the corresponding MOPITT CO (Figure 8), and shows good correlation with the peak CO concentrations over the fire locations (Figure 1). The westward extent of the NO_2 plume over the Atlantic near the equator is not as great as with CO, but neither is this expected since NO_2 has a shorter lifetime. Most of the soil NO_x emissions are also located in the equatorial latitudes over the rain forests of the Congo basin, although the modeling study using MOZART-2 shows these to be dominated by the biomass burning emissions at this time. Significant NO_2 columns over southern Africa are also evident. Soil NO_x emissions are low southward of 10°S, and the fact that there are very few fire counts observed in these regions at this time, together with an absence of significant low altitude CO plumes from MOPITT, points to a lightning source of NO_2. This demonstrates how retrievals from these two sensors may be used together to separate lightning and anthropogenic sources of NO_x. We note that the 'hot spot' of high NO_2 near the Johannesburg metropolitan areas in South Africa is a persistent feature in the GOME data throughout the year [*Velders et al.*, 2001]. An anthropogenic NO_2 column enhancement is also seen at 7°E, 5°N near
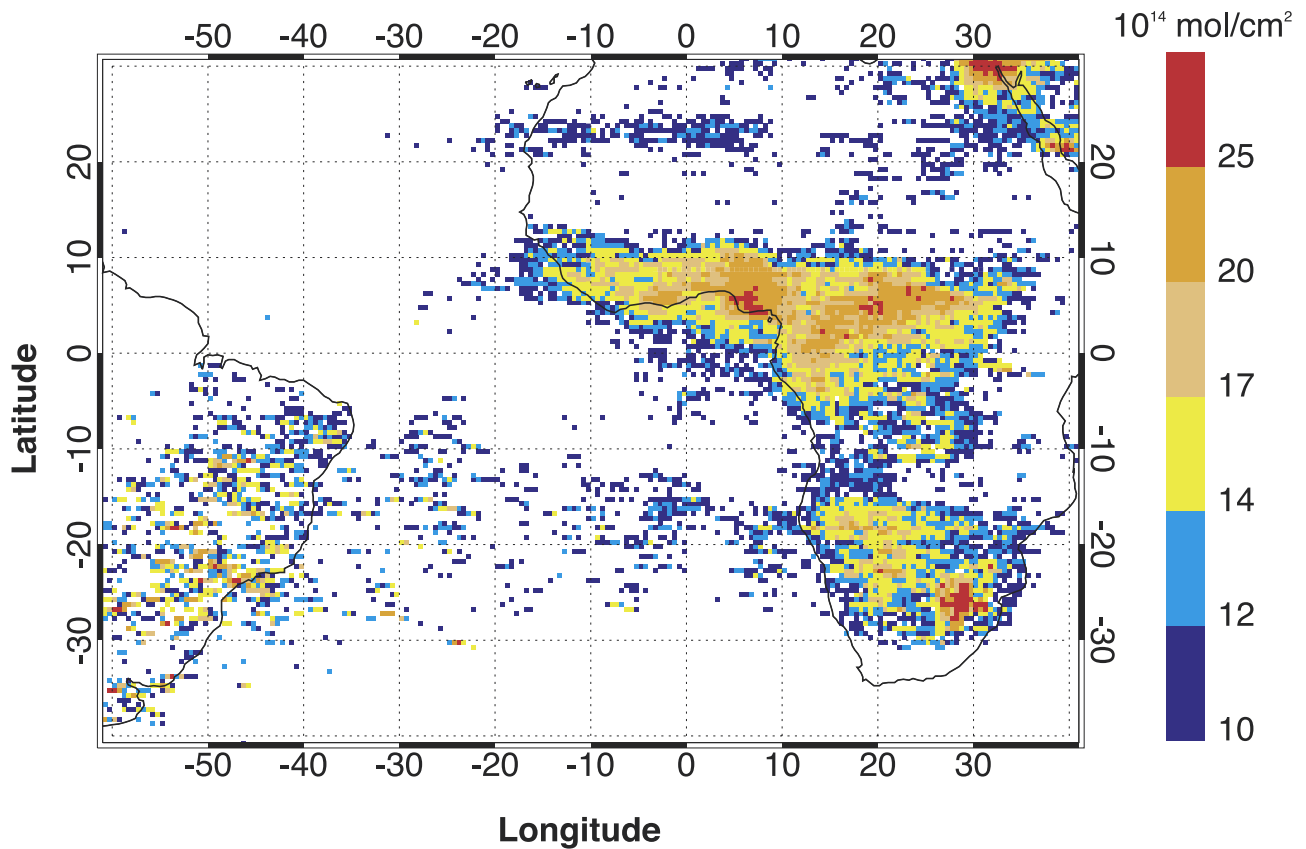
Figure 15. The January 2001 mean GOME residual tropospheric NO_2 vertical column. Data resolution is $0.5°$ longitude $\times$ $0.5°$ latitude.

Lagos, Nigeria. The elevated levels of NO_2 seen over South America are most likely due to a combination of lightning and soil emissions.

[36] Further evidence for the lightning origin of the GOME southern African and South American NO_2 is provided by another instrument on the TRMM satellite, the Lightning Imaging Sensor (LIS) [http://thunder.msfc. nasa.gov/] [*Christian et al.*, 1999]. This sensor employs an optical staring imager which identifies lightning activity by detecting momentary changes in the brightness of the clouds as they are illuminated by lightning discharges. The LIS instrument detects total lightning, since cloud-to-ground, intracloud, and cloud-to-cloud discharges all produce optical pulses that are visible from space. The horizontal resolution is between 3 and 6 km. The January 2001 mean observations of lightning flashes by the TRMM/LIS show significant activity over southern Africa and South America, as shown in Figure 16. The area of highest lightning flash density corresponds reasonably well with the GOME observations of NO_2, although the effect of transport on the monthly mean data should also be considered. Since lightning is associated with strong convection, significant lightning activity is also seen near the ITCZ, especially over the Congo basin. This is consistent with the high levels of NO_2 in this area as noted above, and suggests that in addition to the NO_x produced by the biomass burning and soil emissions, lightning NO_x should also play a significant role in the production of midtroposphere O_3 in the region immediately south of the fires.

[37] To check on our assumption that lightning produces sufficient NO_2, as a fraction of the total NO_x, for detection by GOME, we performed a process study using MOZART-2 for an area of strong model lightning activity over southern Africa, away from the influence of biomass burning and soil emissions. The tropospheric partition of NO_x between NO and NO_2 shows a strong diurnal cycle, with photolysis reducing the NO_2 concentration during the day. The GOME local crossing time was taken into account by using a version of MOZART-2 capable of reporting model fields at a given local time, 1030 in this case, for all locations (C. Granier, Service d'Aéronomie, CNRS, private communication, 2002). The lightning "C-shape" vertical distribution of NO deposition used in the model injects about 15% of the total nitrogen mass below 700 hPa. Here NO_x partitioning favors NO_2, with mixing ratios around 100 pptv. In the midtroposphere, this mixing ratio is reduced to 60 pptv near the peak in the lightning deposition around 350 hPa, while the NO mixing ratio increases to around 200 pptv. This results in representative NO and NO_2 tropospheric columns below the 168 hPa model level of 1.0×10^{15} molecules cm^{-2} and 8.6×10^{14} molecules cm^{-2}, respectively, and we conclude that NO_2 constitutes a significant fraction of the total lightning NO_x. However, the cloud cover associated with lightning activity would mostly obscure this NO_2 from GOME. The actual column measured will likely depend on the NO_2 concentrations that remain after cloud-venting, and might be greatest downwind of storm systems.
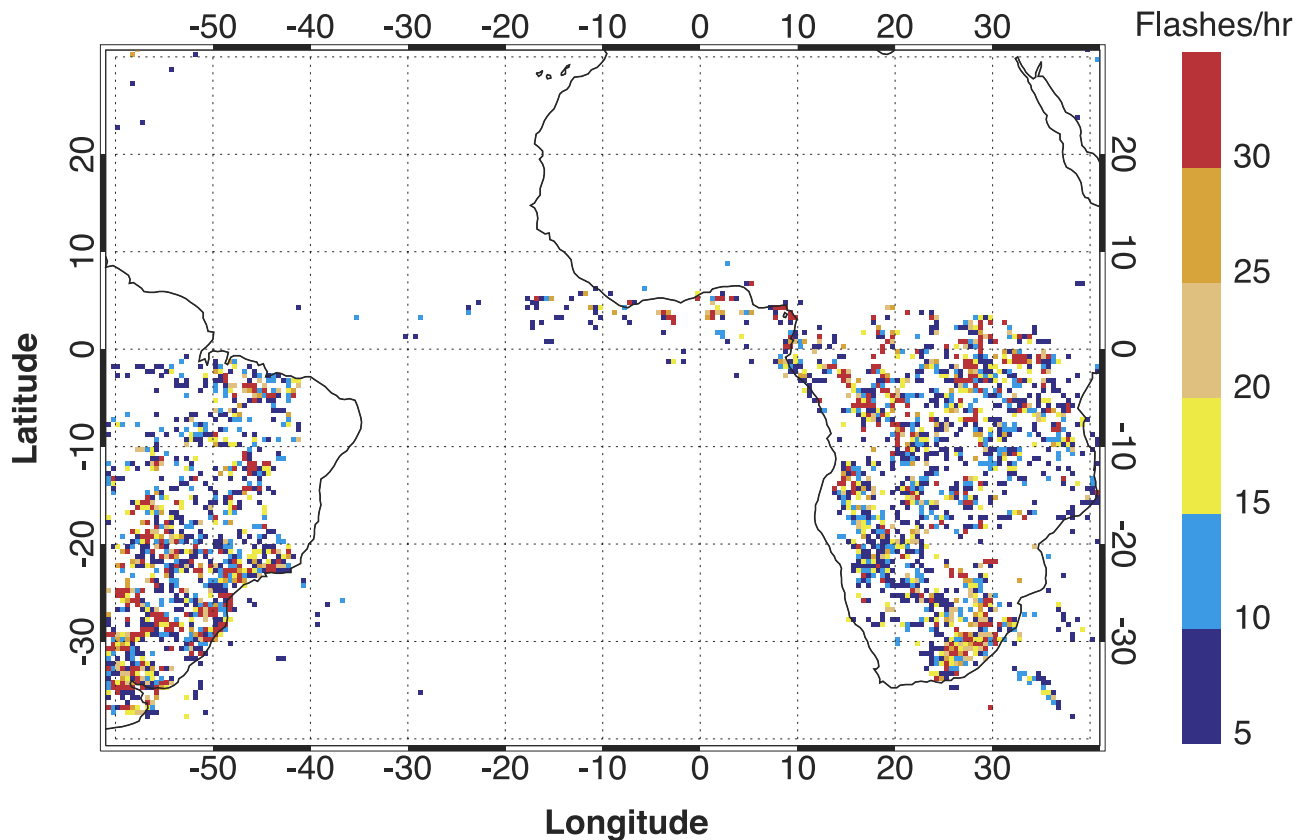
Figure 16. Lightning flash mean count rate detected by the TRMM/LIS instrument for January 2001. Data resolution is 0.5° longitude × 0.5° latitude with a plotting threshold of 5 flashes/hour.

[38] A model validation of the GOME NO_2 measurements is beyond the scope of this paper. However, comparing with Figure 15, we note that the NO_2 column from the model is smaller than that reported by GOME in areas of lightning activity by a factor of about 2. There are several areas of uncertainty in the retrieval of the GOME NO_2 tropospheric residual presented here. The largest of these relate to the calculation of the air-mass factor and cloud effects. The latter is of particular concern, since lightning activity implies significant cloud cover. In general, the presence of cloud will result in an underestimate of NO_2 in the boundary layer and an overestimate above the cloud, by a factor of about 2, due to the increased reflectivity. Using a different air-mass factor calculation and different assumptions about cloud cover corrections than those in the retrievals presented here, *Velders et al.* [2001] also found that MOZART underestimated the average NO_2 over Africa by a factor of 3 compared to their GOME retrieval. Recent work by *Martin et al.* [2002b] to account more accurately for cloud when calculating the air-mass factor and for the assumption of negligible tropospheric NO_2 over the remote oceans, results in retrieved NO_2 columns smaller by a factor of 2 than those of *Velders et al.* [2001]. We are currently investigating the possibility of obtaining information about the height distribution of NO_2 by comparing tropospheric residual columns for GOME clear sky pixels with nearby cloudy pixels [*Richter and Burrows*, 2002]. If clouds are present, NO_2 in the PBL is effectively blocked from view. As a result, only small NO_2 enhancements are observed in the cloudy data over regions of anthropogenic emissions and biomass burning. Conversely, high NO_2 values obtained in cloudy data would suggest a lightning source of NO_x.

7. Conclusions

[39] This study is the first to use information from several tropospheric trace gas satellite sensors to provide a broad picture of the processes affecting tropospheric chemistry and transport. As the data from this new generation of instruments becomes more widely used, we believe they will play an important complementary role to in situ measurements and chemical transport modeling studies in extending our understanding of tropospheric chemistry. In particular, the satellite measurements provide a means to link local production of pollution with regional and global scale tropospheric transport, and in turn, provide a larger spatial and temporal context to point measurements.

[40] Biomass burning is one of the major forcings of tropical tropospheric chemistry. Terra/MOPITT CO plumes correlate well with fire sources as seen by the TRMM/VIRS instrument, and only a short lag time is noted between fire detection and plume observation. This is probably due to vertical transport time, the low sensitivity of the current MOPITT retrieval to the PBL, and the fact that CO is emitted most strongly by smoldering fires which occur after the detection of the flaming stage. Because CO plays such a key role in tropospheric chemistry, and because of its utility

as a tracer of tropospheric transport, observations of this species provide an important window on tropospheric processes.

[41] The measurements of NO_2 from the ERS-2/GOME instrument allow two principal tropical sources of this important O_3 precursor, biomass burning and lightning, to be identified. Good correlation is seen between residual NO_2 tropospheric column retrievals and TRMM/LIS lightning flash observations in southern African regions free of soil emissions, and biomass burning and high CO, thus indicating a lightning source of NO_x. The combination of MOPITT CO, GOME NO_2, and TRMM fire and lightning flash counts provides a powerful tool for investigating the tropospheric production of O_3 precursors.

[42] In this paper, we have used data from different sensors in conjunction with chemical transport modeling with the MOZART-2 CTM to provide a clearer picture of the early year tropical Atlantic tropospheric O_3 distribution, using January 2001 as a case study. Inconsistencies between the various TTO products using EP/TOMS data, and between these products and in situ measurements and modeling, have resulted in much discussion of the apparent tropical O_3 "paradox" or "reversal." This manifests itself as high TTO over the SH Atlantic when the intense biomass burning during this season occurs north of the ITCZ in the NH. Assuming that biomass burning is the main source of the O_3 precursors, this raises the questions of why the peak O_3 columns are not observed close to the fire sources and how the O_3 crosses the ITCZ to reach the SH Atlantic.

[43] On the basis of our analysis of the satellite data and modeling results, we believe the following points to be important in explaining the distribution of tropospheric O_3 over the tropical Atlantic in the early part of the year:

[44] 1. Evidence has previously been presented in the literature that the TOMS TTO retrievals have relatively poor sensitivity to the lower troposphere, and that these products are more indicative of O_3 levels in the mid and upper troposphere. If the O_3 resulting from the NH biomass burning in the early part of the year is concentrated mainly in the lower troposphere, as is suggested by the MOPITT CO profiles, then, with the possible exception of the scan-angle method, the TOMS TTO techniques might not correctly reflect the higher PBL concentrations. This may explain the discrepancy between the TOMS TTO retrievals and modeling studies in which the latter show high O_3 concentrations in the lower troposphere in the vicinity of the NH African fires. This has been noted in previous studies and is also evident in the results presented here. This would be in contrast to the situation during the August–October biomass burning season in southern Africa and South America, when there is evidence that the O_3 plumes reach higher altitudes. In this case, the TOMS TTO over the southern Atlantic appears to correlate more closely with the time and latitudes of the observed burning. During this season, deep convection over Africa is thought to play an important role in raising NO_x to the free troposphere [*Jenkins et al*, 1997], where its lifetime is increased. Associated lightning activity also contributes to NO_x levels, and increases the potential for the local photochemical production of O_3 [*Pickering et al.*, 1996]. In addition, the biomass burning region in Brazil is associated with strong convection which lifts the emissions to the free troposphere

[*Pickering et al.*, 1992]. The Atlantic becomes criss-crossed by free-troposphere plumes moving in opposite directions [*Thompson et al.*, 1996; *Chatfield et al.*, 1998].

[45] 2. High values of lower troposphere CO are measured by MOPITT in the region of the NH fires, and the shape and positions of these plumes correlate well with GOME NO_2 residual column amounts, suggesting that this should be a region of high O_3 production. This is confirmed by biomass burning source perturbation studies using the MOZART-2 CTM.

[46] 3. Using CO as a tracer, the MOPITT profile retrievals indicate that after convection to the free troposphere in the vicinity of the fires, the biomass burning emissions are advected southwest in the Harmattan flow to the position of the ITCZ. Convection and further southern transport occurs over the ITCZ, which has a southern gradient with altitude at this time, especially over eastern Africa. This leads to a CO distribution over the Gulf of Guinea in which the lower troposphere concentration is greatest north of the equator while the mid and upper troposphere latitudinal concentration gradient is reversed. This behavior is observed in the main biomass burning plume that extends from the African continent out into the Atlantic in the latitude band between about 10°N and 10°S. If the O_3 distribution resulting from the fires is assumed to show the same latitudinal characteristics as the CO, then this explains the high-altitude O_3 "reversal" observed in in-situ measurements through the region. However, it is important to note that the main part of this biomass burning plume does not extend far enough south to explain the SH midtropospheric O_3 maximum observed in the TOMS TTO.

[47] 4. Lightning over southern Africa provides a second source of midtroposphere NO_x as shown by the correlation between GOME NO_2 and LIS lightning flash maps. This NO_x combines with CO from NH biomass burning that has reached the SH by the mechanism described above, and forms O_3 in a plume that extends westward out into the Atlantic to the region of the observed TOMS TTO maximum. There is also likely to be a significant contribution from lightning NO_x over South America. This is confirmed by lightning source perturbation studies using the MOZART-2 CTM. The model also suggests that the subsidence of stratospheric air is not an important factor in determining the tropical O_3 maximum, although this cannot be confirmed using the current satellite sensor measurements.

[48] The early year tropical Atlantic O_3 distribution is therefore characterized by two maxima, the first in the lower troposphere, predominantly over the biomass burning region and just to the south of it, and a second in the midtroposphere in the southern tropical Atlantic.

References

Brasseur, G. P., D. A. Hauglustaine, S. Walters, P. J. Rasch, J.-F. Muller, C. Granier, and X. X. Tie, MOZART: A global chemical transport model for ozone and related chemical tracers, Part 1: Model description, *J. Geophys. Res.*, 103, 28,265–28,289, 1998.

Brasseur, G. P., J. J. Orlando, and G. S. Tyndall (Eds.), *Atmospheric Chemistry and Global Change*, chap. 13, pp. 465–486, Oxford Univ. Press, New York, 1999.

Burrows, J. P., et al., The Global Ozone Monitoring Experiment (GOME): Mission concept and first scientific results, *J. Atmos. Sci.*, 56, 151–175, 1999.

Cautenet, S., D. Poulet, C. Delon, R. Delmas, J.-M. Grégoire, J. M. Pereira, S. Cherchali, O. Amram, and G. Flouzat, Simulation of carbon monoxide redistribution over central Africa during biomass burning events (Experiment for Regional Sources and Sinks of Oxidants (EXPRESSO)), *J. Geophys. Res.*, 104, 30,641–30,657, 1999.

Chatfield, R. B., and A. C. Delany, Convection links biomass burning to increased tropical ozone, *J. Geophys. Res.*, 95, 18,473–18,488, 1990.

Chatfield, R. B., J. A. Vastano, L. Li, G. W. Sachse, and V. S. Connors, The Great African plume from biomass burning: Generalizations from a three-dimensional study of TRACE A carbon monoxide, *J. Geophys. Res.*, 103, 28,059–28,077, 1998.

Christian, H. J., et al., The Lightning Imaging Sensor, in *Proceedings of the 11th International Conference on Atmospheric Electricity, NASA Conf. Publ.*, NASA-CP-1999-209261, 746–749, 1999.

Connors, V. S., M. Flood, T. Jones, B. Gormsen, S. Nolf, and H. G. Reichle Jr., Global distribution of biomass burning and carbon monoxide in the middle troposphere during early April and October 1994, in *Biomass Burning and Global Change*, edited by J. S. Levine, pp. 99–106, MIT Press, Cambridge, Mass., 1996.

Deeter, M., L. Emmons, D. P. Edwards, J. Gille, D. Ziskin, J.-L. Attie, J. Warner, J. R. Drummond, L. Yurganov, and P. Noveli, Validation of MOPITT Radiances, *IGARSS '02*, Toronto, Canada, June 24–28 2002.

Drummond, J. R., Measurements of Pollution in the Troposphere (MOPITT), in *The Use of EOS for Studies of Atmospheric Physics*, edited by J. C. Gille and G. Visconti, pp. 77–101, North-Holland, New York, 1992.

Edwards, D. P., C. Halvorson, and J. C. Gille, Radiative transfer modeling for the EOS Terra Satellite Measurement of Pollution in the Troposphere (MOPITT) instrument, *J. Geophys. Res.*, 104, 16,755–16,775, 1999.

Emmons, E., M. Deeter, D. P. Edwards, J. Gille, D. Ziskin, J.-L. Attie, J. Warner, J. R. Drummond, L. Yurganov, P. Novelli, N. Pougatchev, and F. Murcray, Validation of MOPITT retrievals of carbon monoxide, paper presented at IGARSS '02, IEEE, Toronto, Canada, June 24–28 2002.

Fishman, J., and J. C. Larsen, Distribution of total ozone and stratospheric ozone in the tropics: Implications for the distribution of tropospheric ozone, *J. Geophys. Res.*, 92, 6627–6634, 1987.

Fishman, J., V. G. Brackett, E. Browell, and W. B. Grant, Tropospheric ozone derived from TOMS/SBUV measurements during TRACE A, *J. Geophys. Res.*, 101, 24,069–24,082, 1996.

Galanter, M., H. Levy, and G. R. Carmichael, Impacts of biomass burning on tropospheric CO, NO_x, and O_3, *J. Geophys. Res.*, 105, 6633–6653, 2000.

Giglio, G., J. D. Kendall, and C. J. Tucker, Remote sensing of fires with the TRMM VIRS, *Int. J. Remote Sens.*, 21, 203–207, 2000.

Grégoire, J.-M., S. Pinnock, E. Dwyer, and E. Janodet, Satellite monitoring of vegetation fires for EXPRESSO: Outline of activity and relative importance of the study area in the global picture of biomass burning, *J. Geophys. Res.*, 104, 30,691–30,699, 1999.

Hao, W. M., and M.-H. Lui, Spacial and temporal distribution of tropical biomass burning, *Global Biogeochem. Cycles*, 8, 495–504, 1994.

Hauglustaine, D. A., G. P. Brasseur, S. Walters, P. J. Rasch, J.-F. Muller, L. K. Emmons, and M. A. Carroll, MOZART: A global chemical transport model for ozone and related chemical tracers, Part 2: Model results and evaluation, *J. Geophys. Res.*, 103, 28,291–28,335, 1998.

Hauglustaine, D. A., L. K. Emmons, M. Newchurch, G. P. Brasseur, T. Takao, K. Matsubara, J. Johnson, B. Ridley, J. Smith, and J. Dye, On the role of lightning NO_x in the formation of tropospheric ozone plumes: A global model perspective, *J. Atmos. Chem.*, 38, 277–294, 2001.

Hudson, R. D., J.-H. Kim, and A. M. Thompson, On the derivation of tropospheric column from radiances measured by the total ozone mapping spectrometer, *J. Geophys. Res.*, 100, 11,137–11,145, 1995.

Jenkins, G. S., K. Mohr, V. R. Morris, and O. Arino, The role of convective processes over the Zaire-Congo Basin to the Southern Hemispheric ozone maximum, *J. Geophys. Res.*, 102, 18,963–18,980, 1997.

Jonquieres, I., A. Marenco, A. Maalej, and F. Rohrer, Study of ozone formation and transatlantic transport from biomass burning emissions over West Africa during the airborne Tropospheric Ozone Campaigns TROPOZ I and TROPOZ II, *J. Geophys. Res.*, 103, 19,059–19,073, 1998.

Kennedy, P. J., A. S. Belward, and J.-M. Grégoire, An improved approach to fire monitoring in West Africa using AVHRR data, *Int. J. Remote Sens.*, 15, 2235–2255, 1994.

Kim, J. H., M. J. Newchurch, and K. Han, Distribution of tropical tropospheric ozone determined by the Scan-Angle Method applied to TOMS measurement, *J. Atmos. Sci.*, 58, 2699–2708, 2001.

Klenk, K. F., P. K. Bhartia, A. J. Fleig, V. G. Kaveeshwar, R. D. McPeters, and P. M. Smith, Total ozone determination from the Backscatter UV Experiment (BUV), *J. Appl. Meteorol.*, 21, 1672–1684, 1982.

Klonecki, A. A., and H. Levy, Tropospheric chemical ozone tendencies in CO-CH_4-NO_y-H_2O system: Their sensitivity to variations in environmental parameters and their application to a global chemical transport study, *J. Geophys. Res.*, 102, 21,221–21,237, 1997.

Lamarque, J.-F., G. P. Brasseur, P. G. Hess, and J.-F. Mueller, Three-dimensional study of the relative contributions of the different nitrogen sources in the troposphere, *J. Geophys. Res.*, 101, 22,955–22,968, 1996.

Levy, H., W. J. Moxim, A. A. Klonecki, and P. S. Kasibhatla, Simulated tropospheric NO_x: Its evaluation, global distribution, and individual source contributions, *J. Geophys. Res.*, 104, 26,279–26,306, 1999.

Leue, C., M. Wenig, T. Wagner, O. Klimm, U. Platt, and B. Jaehne, Quantitative analysis of NO_x emissions from Global Ozone Monitoring Experiment satellite image sequences, *J. Geophys. Res.*, 106, 5493–5505, 2001.

Lyjak, L. V., and A. K. Smith, Lagrangian mean circulations in the stratosphere, *J. Atmos. Sci.*, 44, 2252–2266, 1987.

Marenco, A., J. C. Medale, and S. Prieur, Study of tropospheric ozone in the tropical belt (Africa, America) from STRATOZ and TROPOZ campaigns, *Atmos. Environ.*, 24A, 2823–2834, 1990.

Marenco, A., et al., Measurement of ozone and water vapor by airbus in-service aircraft: The mozaic airborne program, an overview, *J. Geophys. Res.*, 103, 25,631–25,642, 1998.

Martin, R. V., et al., Interpretation of TOMS observations of tropical tropospheric ozone with a global model and in situ observations, *J. Geophys. Res.*, 107(D18), 4351, doi:10.1029/2001JD001480, 2002a.

Martin, R. V., et al., An improved retrieval of tropospheric nitrogen dioxide from GOME, *J. Geophys. Res.*, 107(D20), 4437, doi:10.1029/2001JD001027, 2002b.

Newchurch, M., D. Sun, X. Liu, J. H. Kim, R. V. Martin, D. Jacob, J. Logan, K. Han, and S. Na, Critical assessment of TOMS-derived tropospheric ozone: Comparisons with other measurements and model evaluation of controlling processes, paper presented at TOMS Science Team Meeting, NASA, Greenbelt, Md., Oct. 2001.

Nielsen, T. T., Characterization of fire regimes in the Experiment for Regional Sources and Sinks of Oxidants (EXPRESSO) study area, *J. Geophys. Res.*, 104, 30,713–30,723, 1999.

Pan, L., J. C. Gille, D. P. Edwards, P. L. Bailey, and C. D. Rodgers, Retrieval of tropospheric carbon monoxide for the MOPITT experiment, *J. Geophys. Res.*, 103, 32,277–32,290, 1998.

Pickering, K. E., A. M. Thompson, J. R. Scala, W.-K. Tao, and J. Simpson, Ozone production potential following convective redistribution of biomass burning emissions, *J. Atmos. Chem.*, 14, 297–313, 1992.

Pickering, K. E., et al., Convective transport of biomass burning emissions over Brazil during TRACE-A, *J. Geophys. Res.*, 101, 23,993–24,012, 1996.

Pickering, K. E., Y. S. Wang, W. K. Tao, C. Price, and J. F. Muller, Vertical distributions of lightning NO_x for use in regional and global chemical transport models, *J. Geophys. Res.*, 103, 31,203–31,216, 1998.

Platt, U., Differential optical absorption spectroscopy (DOAS), in *Air Monitoring by Spectroscopic Techniques*, edited by M. W. Sigrist, pp. 27–84, John Wiley, New York, 1994.

Price, C., and D. Rind, A simple lightning parameterization for calculating global lightning distribution, *J. Geophys. Res.*, 97, 9919–9933, 1992.

Reichle, H. G., Jr., V. S. Connors, J. A. Holland, R. T. Sherrill, H. A. Wallio, J. C. Casas, E. P. Condon, B. B. Gormsen, and W. Seiler, The distribution of middle tropospheric carbon monoxide during early October 1984, *J. Geophys. Res.*, 95, 9845–9856, 1990.

Richter, A., and J. P. Burrows, Retrieval of Tropospheric NO_2 from GOME Measurements, *Adv. Space Res.*, 29, 1673–1683, 2002.

Ridley, B. A., S. Madronich, R. B. Chatfield, J. G. Walega, R. E. Shetter, M. A. Carroll, and D. D. Montzka, Measurements and model simulations of the photostationary state during the Mauna Loa Observatory Photochemistry Experiment: Ozone production and loss rates, *J. Geophys. Res.*, 97, 10,275–10,388, 1992.

Rodgers, C. D., *Inverse Methods for Atmospheric Sounding*, World Sci., River Edge, N. J., 2000.

Scott, R. K., J.-P. Cammas, P. Mascart, and C. Stolle, Stratospheric filamentation into the upper tropical troposphere, *J. Geophys. Res.*, 106, 11,835–11,848, 2001.

Siegert, F., A. Hoffman, and S. Kuntz, Comparison of ATSR and NOAA AVHRR hotspot data acquired during an exceptional fire event in Kalimantan (Indonesia), paper presented at International Workshop on Applications of the ERS ATSR, ESRIN, Italy, 23–25 June 1999.

Thompson, A. M., and R. D. Hudson, Tropical tropospheric ozone (TTO) maps from Nimbus 7 and Earth-Probe TOPS by the modified-residual method: Evaluation with sondes, ENSO signals, and trends from Atlantic regional time series, *J. Geophys. Res.*, 104, 26,961–26,975, 1999.

Thompson, A. M., K. E. Pickering, D. P. McNamara, M. R. Schoeberl, R. D. Hudson, J. H. Kim, E. V. Browell, V. W. J. H. Kirchhoff, and D. Nganga, Where did tropospheric ozone over southern Africa and the tropical Atlantic come from in October 1992?: Insights from TOMS, GTE TRACE A, and SAFARI 1992, *J. Geophys. Res.*, 101, 24,251–24,278, 1996.

Thompson, A. M., B. G. Dodderidge, J. C. White, R. D. Hudson, W. T. Luke, J. E. Johnson, B. J. Johnson, S. J. Oltmans, and R. Weller, A tropical Atlantic paradox: Shipboard and satellite views of a tropospheric ozone maximum and wave-one in January–February 1999, *Geophys. Res. Lett.*, 27, 3317–3320, 2000.

Thompson, A. M., J. C. Witte, R. D. Hudson, H. Guo, J. R. Herman, and M. Fujiwara, Tropical tropospheric ozone and biomass burning, *Science*, 291, 2128–2132, 2001.

Tie, X., R. Zhang, G. Brasseur, L. Emmons, and W. amd Lei, Effects of lightning on reactive nitrogen and nitrogen resevoir speices in the troposphere, *J. Geophys. Res.*, 106, 3167–3178, 2001.

Velders, G. J., C. Granier, R. W. Portmann, K. Pfeilsticker, M. Wenig, T. Wagner, U. Platt, A. Richter, and J. P. Burrows, Global tropospheric NO$_2$ column distributions: Comparing three-dimensional model calculations with GOME measurements, *J. Geophys. Res.*, 106, 12,643–12,660, 2001.

Wang, Y., D. J. Jacob, and J. A. Logan, Global simulation of tropospheric O$_3$-NO$_x$-hydrocarbon chemistry, 1, Model formulation, *J. Geophys. Res.*, 103, 10,713–10,725, 1998.

Wang, Y., S. C. Liu, H. Yu, S. T. Sandholm, T. Chen, and D. R. Blake, Influence of convection and biomass burning outflow on tropospheric chemistry over the tropical Pacific, *J. Geophys. Res.*, 105, 9321–9333, 2000.

Watson, C. E., J. Fishman, and H. G. Reichle Jr., The significance of biomass burning as a source of carbon monoxide and ozone in the southern hemisphere tropics: A satellite analysis, *J. Geophys. Res.*, 95, 16,443–16,450, 1990.

Ziemke, J. R., S. Chandra, and P. K. Bhartia, Two new methods for deriving tropospheric column ozone from TOMS measurements: Assimilated UARS MLS/HALOE and convective-cloud differential techniques, *J. Geophys. Res.*, 103, 22,115–22,127, 1998.

————————————

J.-L. Attié and J.-P. Cammas, Laboratoire d'Aérologie, Observatoire Midi Pyrénées, 14 Avenue E. Belin, 31400 Toulouse, France. (attjl@aero.obs-mip.fr; camjp@aero.obs-mip.fr)

J. P. Burrows and A. Richter, Institute of Environmental Physics, University of Bremen, P. O. Box 33 04 40, D-28334 Bremen, Germany. (burrows@iup.physik.uni-bremen.de; Andreas.Richter@iup.physik.uni-bremen.de)

M. N. Deeter, D. P. Edwards, L. K. Emmons, G. L. Francis, J. C. Gille, J.-F. Lamarque, L. V. Lyjak, J. Warner, and D. C. Ziskin, National Center for Atmospheric Research, P.O. Box 3000, Boulder, CO 80307-3000, USA. (mnd@ucar.edu; edwards@ucar.edu; emmons@ucar.edu; gfrancis@ucar.edu; gille@ucar.edu; lamar@ucar.edu; lvl@ucar.edu; juying@ucar.edu; ziskin@ucar.edu)

J. R. Drummond, Department of Physics, University of Toronto, Department of Physics, Saint George Street, Toronto, Ontario M5S 1AS, Canada. (jim@atmosp.physics.utoronto.ca)